WATER RESOURCES RESEARCH, VOL. 27, NO. 12, PAGES 3075–3094, DECEMBER 1991

A Model for Simulating Transport of Reactive Multispecies Components: Model Development and Demonstration

GOUR-TSYH YEH

Department of Civil Engineering, Penn State University, University Park, Pennsylvania

VIJAY S. TRIPATHI

Science Applications International Corporation, McLean, Virginia

This paper presents the development and demonstration of a two-dimensional finite-element hydrogeochemical transport model, HYDROGEOCHEM, for simulating transport of reactive multispecies solutes. The model is designed for application to heterogeneous, anisotropic, saturated-unsaturated media under transient or steady state flow conditions. It simulates the chemical processes of complexation, dissolution-precipitation, adsorption-desorption, ion exchange, redox, and acid-base reaction, simultaneously. A set of four example problems are presented. The examples illustrate the model's ability to simulate a variety of reactive transport problems. Important results presented include a depiction of the propagation of multiple precipitation-dissolution fronts, a display of the large errors in model response if the number of iterations between the hydrologic transport and chemical equilibrium modules is limited to one, an illustration of the development of greater concentration of contaminants in groundwater away from a waste site than near the source, and a demonstration of the variation in distribution coefficients of more than 6 orders of magnitude.

INTRODUCTION

During subsurface transport, reactive solutes are subject to a variety of hydrophysical and chemical processes. The major hydrophysical processes include advection and convection, dispersion and diffusion, compaction and consolidation, and radioactive decay. The key chemical processes are complexation including hydrolysis and acid-base reactions, oxidation-reduction, dissolution-precipitation, adsorption, and ion exchange. The combined effects of all these processes on solute transport must satisfy the principle of conservation of mass. The statement of conservation of mass for N components leads to N partial differential equations (PDEs). Traditional solute transport models often incorporate the effects of hydrophysical processes rigorously but oversimplify chemical interactions among aqueous species, and account for heterogeneous reactions with empirical approaches such as the linear (K_d approach) and nonlinear (Freundlich) isotherms (for example, see *Yeh and Huff* [1985] and *Huyakorn et al.* [1985]). Sophisticated chemical equilibrium models, on the other hand, incorporate a variety of chemical processes but assume a no-flow (batch) system [*Morel and Morgan*, 1972; *Truesdell and Jones*, 1974; *Westall et al.*, 1976; *Parkhurst et al.*, 1980].

In past decade, coupled models accounting for complex hydrophysical and chemical processes, with varying degrees of sophistication, have been developed [*Grove and Wood*, 1979; *Valocchi et al.*, 1981; *Jennings et al.*,1982; *Schulz and Reardon*, 1983; *Walsh et al.*, 1984; *Cederberg*, 1985; *Kirkner et al.*, 1985; *Lichtner*, 1985; *Bryant et al.*, 1986; *Lewis et al.*, 1987; *Hostetler et al.*, 1989; *Liu and Narasimhan*, 1989*a*, *b*; *Yeh and Tripathi*, 1990]. The existing models of reactive transport employ two basic sets of equations. The transport of solutes is described by a set of partial differential equations (PDEs), and the chemical processes, under the assumption of equilibrium, are described by a set of nonlinear algebraic equations (AEs). Three major approaches have been used to solve the problem [*Yeh and Tripathi*, 1989]: (1) considering the system as a set of simultaneous mixed differential and algebraic equations (DAEs), (2) using direct substitution of nonlinear chemical reactions into the transport equations to reduce the system to a set of nonlinear PDEs, and (3) considering the system as coupled sets of sequential linear PDEs and nonlinear AEs. An important consideration in any approach is the choice of primary dependent variables (PDVs) in transport equations. Once PDVs are obtained, secondary dependent variables (SDVs) and their partial derivatives with respect to PDVs can be computed analytically or numerically from chemical reaction equations. Many models, in recent years, have been developed using a combination of these three approaches. Most of these models cannot account for the complete set of chemical processes, cannot be easily extended to include mixed chemical equilibria and kinetics, and cannot handle practical two- and three-dimensional problems [*Yeh and Tripathi*, 1989]. The difficulties arise mainly from improper selection of PDVs in the transport equations. The advantages and disadvantages of various types of models were discussed elsewhere [*Yeh and Tripathi*, 1989]. This paper presents the development and demonstration of a hydrogeochemical transport model of reactive multispecies chemicals. It employs total analytical concentration of components as the PDVs. The entire system of equations comprises a coupled, sequential set of linear PDEs and nonlinear AEs.

Paper number 91WR02028.
0043-1397/91/91WR-02028$05.00

STATEMENT OF GOVERNING EQUATIONS

Hydrologic Transport Equations

The transport equations for N_a aqueous components, N_s adsorbent components, and the cation exchange capacity

can be derived based on the principle of conservation of mass. The derivation of these transport equations can be found elsewhere [*Yeh and Tripathi*, 1990]:

$$\theta \frac{\partial T_j}{\partial t} + \frac{\partial \theta}{\partial t}(S_j + P_j) + \mathbf{V} \cdot \nabla C_j = \nabla \cdot \theta \mathbf{D} \cdot \nabla C_j + Q C_j^* - Q C_j - \lambda_j^a T_j \qquad j = 1, 2, \cdots, N_a \quad (1)$$

$$\theta \frac{\partial W_j}{\partial t} + \frac{\partial \theta}{\partial t} W_j = M_j - \lambda_j^s W_j \qquad j = 1, 2, \cdots, N_s \quad (2)$$

$$\theta \frac{\partial N_{eq}}{\partial t} + \frac{\partial \theta}{\partial t} N_{eq} = M_{eq} - \lambda_{eq} N_{eq} \quad (3)$$

in which

$$C_j = c_j + \sum_{i=1}^{M_x} a_{ij}^x x_i \qquad j = 1, 2, \cdots, N_a \quad (4)$$

$$S_j = \sum_{i=1}^{M_y} a_{ij}^y y_i + \sum_{i=1}^{M_z} a_{ij}^z z_j \qquad j = 1, 2, \cdots, N_a \quad (5)$$

$$P_j = \sum_{i=1}^{M_p} a_{ij}^p p_i \qquad j = 1, 2, \cdots, N_a \quad (6)$$

$$T_j = c_j + \sum_{i=1}^{M_x} a_{ij}^x x_i + \sum_{i=1}^{M_y} a_{ij}^y y_i + \sum_{i=1}^{M_z} a_{ij}^z z_i + \sum_{i=1}^{M_p} a_{ij}^p p_i \qquad j = 1, 2, \cdots, N_a \quad (7)$$

$$W_j = s_j + \sum_{i=1}^{M_y} b_{ij}^y y_i \qquad j = 1, 2, \cdots, N_s \quad (8)$$

$$N_{eq} = \sum_{i=1}^{M_z} \nu_i z \quad (9)$$

where θ is the moisture content (L^3/L^3); t is the time (T); T_j, S_j, P_j, and C_j are the total analytical (dissolved, sorbed, and precipitated) concentration, total sorbed (adsorbed and ion-exchanged) concentration, total precipitated concentration, and total dissolved concentration, respectively, of the jth aqueous component (M/L^3); $\mathbf{V}$ is the Darcy velocity (L/T); $\mathbf{D}$ is the dispersion coefficient tensor (L^2/T); Q_j (L^3/T) is the flow rate of artificial injection and C_j^* (M/L^3) is the concentration of the jth component in the source of injecting water; λ_j^a is the decay rate constant of the jth aqueous component ($1/L$); N_a is the number of aqueous components; W_j is the total analytical concentration of the jth adsorbent component (M/L^3); M_j is the artificial source of the jth adsorbent component; λ_j^s is the decay constant of the jth adsorbent component; N_s is the number of adsorbent components; N_{eq} is the number of equivalents of the cation exchange sites per liter of solution (M/L^3); M_{eq} is the number of equivalents added to the system; λ_{eq} is the decay constant of the cation exchange sites; c_j is the concentration of the jth aqueous component species (M/L^3); x_i is the concentration of the ith complexed species (M/L^3); a_{ij}^x is the stoichiometric coefficient of the jth aqueous component in the ith complexed species; M_x is the number of complexed species; y_i is the concentration of the ith adsorbed species (M/L^3); a_{ij}^y is the stoichiometric coefficient of the jth aqueous component in the ith adsorbed species; M_y is the number of adsorbed species; z_i is the concentration of the ith ion-exchanged species (M/L^3); a_{ij}^z is the stoichiometric coefficient of the jth aqueous component in the ith ion-exchanged species; M_z is the number of ion-exchanged species; p_i is the concentration of the ith precipitated species (M/L^3); a_{ij}^p is the stoichiometric coefficient of jth aqueous component in the ith precipitated species; M_p is the number of precipitated species; s_j is the concentration of the jth adsorbent component species (M/L^3); b_{ij}^y is the stoichiometric coefficient of the jth adsorbent component in the ith adsorbed species; and ν_i is the charge of the ith ion-exchanged species.

Equations (1)–(8) constitute eight sets of equations in 12 sets of unknowns (T_j, C_j, S_j, P_j, c_j, W_j, s_j, N_{eq}, x_i, y_i, z_i, and p_i); hence the formulation is not complete. Four sets of constitutive relationships among those unknowns must be established to complete the formulation. A chemical equilibrium model is adopted to give the implicit functional relationships among T_j, C_j, S_j, P_j, c_j, W_j, s_j, N_{eq}, x_i, y_i, z_i, and p_i variables as described in the following section.

Chemical Equilibrium Equations

Chemical reactions are described by a set of nonlinear algebraic equations under the assumption of local equilibrium. These equations are obtained based on the law of mass action [*Westall et al.*, 1976].

Aqueous complexation. Equations for aqueous complexation are obtained using the law of mass action as follows:

$$x_i = \alpha_i^x \prod_{k=1}^{N_a} c_k^{a_{ik}^x} \qquad i = 1, 2, \cdots, M_x \quad (10a)$$

in which

$$\alpha_i^x = K_i^x \prod_{k=1}^{N_a} (\gamma_k^a)^{a_{ik}^x} / \gamma_i^x \qquad i = 1, 2, \cdots, M_x \quad (10b)$$

where α_i^x is the stability constant (at ionic strength, $I \neq 0$) of the ith complexed species, K_i^x is the thermodynamic equilibrium constant of the ith complexed species, γ_i^x is the activity coefficient of the ith complexed species (L^3/M), and γ_j^a is the activity coefficient of the jth aqueous component species (L^3/M).

Adsorption reactions. Equations for adsorption equilibria are obtained using the law of mass action as follows:

$$y_i = \alpha_i^y \left(\prod_{k=1}^{N_a} c_k^{a_{ik}^y} \right) \left(\prod_{k=1}^{N_s} s_k^{b_{ik}^y} \right) \qquad i = 1, 2, \cdots, M_y \quad (11a)$$

in which

$$\alpha_i^y = K_i^y \left[\prod_{k=1}^{N_a} (\gamma_k^a)^{a_{ik}^y} \right] \left[\prod_{k=1}^{N_s} (\gamma_k^s)^{b_{ik}^y} \right] \Big/ \gamma_i^y \qquad i = 1, 2, \cdots, M_y \quad (11b)$$

where a_i^y is the stability constant (at $I \neq 0$) of the ith adsorbed species, K_i^y is the equilibrium constant of the ith adsorbed species, γ_i^y is the activity coefficient of the ith adsorbed species (L^3/M), and γ_j^y is the activity coefficient of the jth adsorbent component species (L^3/M).

Ion exchange. Equations governing ion exchange reactions are obtained as follows:

$$z_i = [\kappa_{iJ} z^{\nu_i} (a_i^{\nu_J} / a_J^{\nu_i})(s_T)^{\nu_J - \nu_i}]^{1/\nu_J} \qquad (12a)$$

$$i = 1, 2, \cdots, M_z$$

in which

$$\kappa_{iJ} = K_{iJ} \gamma_i^{\nu_J} / \gamma_J^{\nu_i} \qquad (12b)$$

$$s_T = \sum_{i=1}^{M_z} z_i \qquad i = 1, 2, \cdots, M_z \qquad (12c)$$

where κ_{iJ} is the selectivity coefficient (at $I \neq 0$), K_{iJ} ($K_{JJ} = 1$) is the selectivity coefficient (at $I = 0$) of the ith species with respect to the Jth species or the effective equilibrium constant of ith ion-exchanged species, ν_i is the charge of the ith ion-exchanged species, γ_i is the activity coefficient of the ith aqueous species denoting either γ_i^x or γ_j^a (L^3/M), a_i is the molar concentration of the ith aqueous species denoting either c_j or x_i (M/L^3), z_i is the molar concentration of the ith ion-exchanged species, denoting either exchanged c_j or x_i (M/L^3), s_T is the total concentration of all ion-exchanged species (M/L^3), and N_{eq} is the number of equivalents per unit solution volume for ion exchange. It should be noted that in deriving (12*a*) the activity of any ion-exchanged species is assumed to be proportional to its molar concentration. Equations (9) and (12*a*) constitute M_z equations for M_z unknown z_i. For homovalent exchange, substituting (9) into (12*a*), and with adequate mathematical manipulation, one can explicitly obtain concentrations of every ion-exchanged species in terms of aqueous component species concentrations and the ion exchange site [*Valocchi et al.*, 1981]. For general heterovalent exchange, it is very difficult to derive such an analytical expression for the concentrations z_i, and numerical evaluations of z_i in terms of c_j are normally used.

Precipitation-dissolution. Equations for precipitation-dissolution are obtained using the law of mass action for each mineral as follows:

$$1 = \alpha_i^p \prod_{k=1}^{N_a} c_k^{a_{ik}^p} \qquad i = 1, 2, \cdots, M_p \qquad (13a)$$

in which

$$\alpha_i^p = K_i^p \prod_{k=1}^{N_a} (\gamma_k^a)^{a_{ik}^p} \qquad i = 1, 2, \cdots, M_p \qquad (13b)$$

where α_i^p is the stability constant (at $I \neq 0$) of the ith precipitated species and K_i^p is the thermodynamic equilibrium constant of the ith precipitated species. Equation (13) does not contain the precipitated molar concentration p_i because the activity of pure solids is considered 1. The absence of p_i in (13) characterizes the chemical reaction of precipitation-dissolution and distinguishes it from other heterogeneous classes of chemical reactions such as adsorption and ion exchange, and from homogeneous complexation reactions. This follows from the fact that for solid phases (activity equals 1) the thermodynamic equilibria do not specify the mass of the solid [*Stumm and Morgan*, 1981], and implies that models developed specifically for handling complexation and sorption cannot simulate dissolution-precipitation.

The thermodynamic equilibrium constants, K_i^x, K_i^y, K_{iJ}, and K_i^p, depend on the temperature and pressure of the system [*Stumm and Morgan*, 1981]. They are normally given for conditions of temperature equal to 25°C and pressure equal to 1 atm. Under other conditions, the thermodynamic equilibrium constants must be corrected for temperature and pressure [*Truesdell and Jones*, 1974]. Similarly, stability constants must be corrected for nonzero solution ionic strength via activity coefficients. The activity coefficients γ_i^y of all adsorbed species are assumed to be one, whereas the activity coefficients γ_k^a and γ_i^x of all aqueous species are calculated using the Davies equation for ionic strength up to 0.3 M [*Stumm and Morgan*, 1981]. When ionic strength is higher, other models of activity coefficient correction should be used. This can easily be done as HYDROGEOCHEM was designed in modular format [*Yeh and Tripathi*, 1990]. The ionic strength of the system is simply equal to one half of the summation of the product of species concentration and the square of the valence over all aqueous species. Thus the stability constants, α_i^x, α_i^y, κ_{iJ}, and α_i^p, are functions of temperature, pressure, and concentrations of all aqueous species.

Redox reactions and electron activity. Redox reactions involve transfer of electrons. In considering such reactions, we must invoke the principle of conservation of electrons to ensure that all electrons donated by chemical species are accepted by other species. Using the concept of "operational" electrons [*Yeh and Tripathi*, 1989], one can consider an electron as an aqueous component with its activity as a master variable. Thus no special mathematical treatment is needed for redox reactions [*Reed*, 1982]. Additionally, a redox reaction can be considered as a complexation or precipitation reaction if the resulting chemical species is an aqueous species or a precipitated solid. Similarly, a redox reaction can be considered as an adsorption reaction or an ion exchange reaction if the resulting species is a surface species. Redox reactions, however, require special numerical consideration. This point will be discussed later on.

Acid-base reactions and proton activity. Acid-base reactions involve transfer of protons. Examples include protonation, hydrolysis, etc. [*Stumm and Morgan*, 1981]. In a system involving acid-base reactions, an additional parameter describing the acidity of the system is needed. This additional parameter is the proton activity (pH). The pH may be computed by using either the electroneutrality or the proton condition. These two approaches are mathematically, but not computationally, equivalent [*Morel and Morgan*, 1972]. In coupling the hydrologic transport and chemical equilibria, it is preferable to use the proton condition approach. In the proton condition approach, the total concentration of the excess proton ($\Sigma H+ - \Sigma OH^-$) must be known before the pH can be computed. Thus if one considers the proton as an aqueous component and defines the mole balance of this component based on "excess" proton concentration, then mathematically no special treatment is needed for acid-base reactions; this approach has been used by numerous previous researchers [*Westall et al.*, 1976]. An acid-base reaction can be considered an aqueous complexation or a precipitation reaction if the resulting species containing H^+ or OH^- ions is an aqueous species or a precipitated species. Similarly, an acid-base reaction can be

considered as an adsorption or ion exchange reaction if the resulting species containing H^- or OH^- ions is a surface species. Numerically, acid-base reactions require some minor special consideration. This point will be discussed later.

From the above discussion, it is seen that although the full complement of geochemical reactions considered here includes complexation, adsorption, ion exchange, precipitation-dissolution, redox, and acid-base reactions, the term "full complement" is meant to include only the first four types of reactions because the latter two reactions require no special treatment mathematically. Numerically, they require special attention as shall be seen later.

Equations (1)–(13) form 12 sets (equations (9) and (12) form a set for M_z z_i variables) of equations and contain 12 sets of unknowns (C_j, S_j, P_j, T_j, W_j, N_{eq}, x_i, c_i, y_i, z_i, s_i and p_i). This system of equations represents hydrologic transport and chemical processes of acid-base reactions, complexation, redox, dissolution-precipitation, adsorption, and ion exchange. Depending on the processes of chemical equilibrium considered, there may be many ways to mathematically reduce the system of equations and thereby simplify the analysis [*Rubin*, 1983].

Currently, there are three approaches to modeling coupled hydrologic transport and geochemical reactions at equilibrium: (1) the differential and algebraic equations (DAE) approach in which the transport equations and chemical reaction equations are solved simultaneously as a system, (2) the direct substitution approach (DSA) in which the chemical reaction equations are substituted into the transport equations to form a highly nonlinear system of partial differential equations, and (3) the sequential iteration approach (SIA) in which the hydrologic transport equations and chemical equilibrium equations are considered two subsystems. An extremely important consideration in any approach is the choice of the PDVs, which determines whether the approach can deal with the complete suite of chemical reactions, how practically it can be used for realistic two- and three-dimensional applications, and how easily it can be extended to handle chemical kinetics. PDVs are defined in this paper as the variables that are solved for via primary governing equations, rather than via secondary governing equations. Any variable that is solved for via a secondary governing equation is termed a secondary dependent variable (SDV). The choice of PDVs and SDVs from T_j, C_j, S_j, P_j, c_k, W_j, s_k, N_{eq}, x_i, y_i, z_i, and p_i is equivalent to partitioning of (1)–(13) into two systems. One system consists of the primary governing equations (PGEs), which are mainly hydrologic transport equations. The other consists of secondary governing equations (SGEs), which are mainly chemical reaction equations.

Both DAE and DSA approaches require simultaneous solution of a significant number of field equations (equations include spatial derivatives, hence transport) and thus are too computer-intensive for realistic two- and three-dimensional applications [*Yeh and Tripathi*, 1989]. We observe that only the PDEs governing the chemical transport are the field equations. The ordinary differential equations (ODEs) governing the change in total adsorbent concentrations and ion exchange sites, and the nonlinear AEs governing chemical equilibrium reactions are point equations (equations that do not include spatial derivatives and hence are applicable to batch systems only). Furthermore, each transport equation for a component is identical in form. This suggests that once the PDVs are chosen for the set of transport equations, they can be solved one by one independently of each other, one each for the associated PDV. All other secondary dependent variables (SDVs) can be obtained from the set of chemical equilibrium reaction and molar balance equations. This approach of iterating between sequentially (not simultaneously as done in DSA models) solving transport equations and solving geochemical equilibria provides perhaps the best hope for realistic, practical two- and three-dimensional applications in terms of requirements for computer resources. This approach is taken in this work.

Using the SIA approach, we may choose (1) concentrations of aqueous component species as PDVs, (2) total dissolved concentrations of aqueous components as PDVs, or (3) total analytical concentrations of aqueous components as PDVs. Using the first two types of PDVs, we cannot include precipitation-dissolution reactions [*Yeh and Tripathi*, 1989]. Hence the total analytical concentrations, T_j, of aqueous components will be chosen as PDVs. For the models that use the T_j as PDVs, the hydrologic transport equations can be written in the explicit form [*Walsh et al.*, 1984; *Cederberg*, 1985; *Bryant et al.*, 1986] as

$$\theta \frac{\partial T_j}{\partial t} + \frac{\partial \theta}{\partial t} T_j = L(C_j) + \frac{\partial \theta}{\partial t} C_j + Q(C_j^* - C_j) \qquad (14)$$

$$j = 1, 2, \cdots, N_a$$

or in the implicit form

$$\theta \frac{\partial T_j}{\partial t} + \frac{\partial \theta}{\partial t} T_j - \mathcal{L}(T_j) = -\mathcal{L}(S_j + P_j) + QC_j^* \qquad (15a)$$

$$j = 1, 2, \cdots, N_a$$

in which L is the advection-dispersion operator representing hydrologic transport and

$$\mathcal{L}(\ \ ) = \left(-V \cdot \nabla + \nabla \cdot \theta \mathbf{D} \cdot \nabla - Q + \frac{\partial \theta}{\partial t}\right)(\ \ ) \qquad (15b)$$

Either of equations (14) or (15) constitutes the subsystem of PGEs for PDVs T_j whereas (2)–(13) constitute the subsystem of SGEs for SDVs C_j, S_j, P_j, c_j, W_j, s_j, N_{eq}, x_i, y_i, z_i, and p_i. The sequence of iterating the PGEs (equation (14)) and the SGEs (equations (2)–(13)) has been well documented [*Walsh et al.*, 1984; *Cederberg*, 1985; *Bryant et al.*, 1986] and will not be repeated here. Using the implicit form of the hydrologic transport equation, we perform similar iteration procedures. A computer program, HYDROGEOCHEM [*Yeh and Tripathi*, 1990], was developed to implement these iteration procedures.

In solving (14) or (15), one substitutes the known values of previous iteration C_j^k or S_j^k and P_j^k for the terms on the right-hand side and solves for the unknown values of the present iteration $T_j^{(k+1)}$ for the terms on the left-hand side. Thus it can be seen that $T_j^{(k+1)}$ values computed with (14) are prone to negative concentrations if $L(C_j^k)$ on the right-hand side is negative. On the other hand, even if $-L(S_j^k + P_j^k)$ on the right-hand side of (15) is negative, the $T_j^{(k+1)}$ values obtained with (15) are not necessarily negative because the term $-L(T_j^{(k+1)})$ can yield a larger negative value than that resulting from the operation of $-L$ on $(S_j^k + P_j^k)$ and make the solution $T_j^{(k+1)}$ values positive. This intuitive observa-

tion is confirmed later in the example problems for demonstration.

The explicit form, (14), cannot be used to solve for the steady state concentration distribution in a one-step iteration. For a one-step solution, one simply sets the time derivative term equal to zero. If this is done, the PDVs disappear from (14) and one is left with nothing to solve for. To reach a steady state solution with the explicit modeling, one has to proceed with many time step iterations. On the other hand, for the implicit form, (15), we simply set the time derivative term on the left-hand side equal to zero and iterate between the simplified (15) and the remaining governing equations, (2)–(13).

To complete the description of the hydrologic transport as given by (1) and mass conservation for adsorbent and ion exchange sites as given by (2) and (3), respectively, initial and boundary conditions must be specified in accordance with physiochemical considerations. It will be assumed that initially the total analytical concentrations for all components and the number of equivalents of the ion exchange site are known throughout the region of interest, i.e.,

$$T_j = T_{j0} \text{ at } t = 0 \qquad j = 1, 2, \cdots, N_a \tag{16}$$

$$W_j = W_{j0} \text{ at } t = 0 \qquad j = 1, 2, \cdots, N_s \tag{17}$$

$$N_{eq} = N_{eq0} \text{ at } t = 0 \tag{18}$$

where T_{j0} is the initial total analytical concentration of the jth aqueous component (M/L^3), W_{j0} is the initial total analytical concentration of the jth adsorbent component (M/L^3), and N_{eq0} is the initial number of equivalents of the ion exchange site (M/L^3). Initial concentrations for aqueous components may be obtained from field measurements or by solving the steady state version of (1) with time invariant boundary conditions.

The specification of boundary conditions is the most difficult and intricate task in multicomponent transport modeling. From a dynamic point of view, a boundary segment may be classified as flow-through or impervious. From a physical point of view, it is a soil-air interface, or soil-soil interface, or soil-water interface. From the mathematical point of view, it may be treated as a Dirichlet boundary on which the total analytical concentration is prescribed, or a Neumann boundary on which the flux due to the gradient of total analytical concentration is known, or a Cauchy boundary on which the total flux is given. Another type of mathematical boundary is the variable conditions on which either Neumann or Cauchy conditions may prevail and which may change with time. These boundary conditions are often specified in view of the hydrogeochemical setting under consideration.

Regardless of the point of view chosen, all boundary conditions eventually must be transformed into mathematical equations for quantitative simulations. Thus we will specify the boundary conditions from the mathematical point of view in concert with dynamic and physical considerations. The boundary conditions imposed on any segment of the boundary are taken to be either Dirichlet or variable for T_j with $j = 1, 2, \cdots, N_a$ independently of each other. The conditions imposed on the Dirichlet boundaries are given as

$$T_j = T_{jD} \text{ on } B_D \qquad j = 1, 2, \cdots, N_a \tag{19}$$

where T_{jD} is the prescribed Dirichlet total analytical concentration (M/L^3), and B_D is the Dirichlet boundary segment.

The conditions imposed on the variable-type boundary, which is normally the soil-air interface or soil-water interface, are either the Neumann with zero gradient flux or the Cauchy with given total flux. The former is specified when the water flow is directed out of the region from the far away boundary whereas the latter is specified when the water flow is directed into the region. This type of variable condition would normally occur at flow-through boundaries. Written mathematically, the variable boundary condition is given by

$$-\mathbf{n} \cdot \theta \mathbf{D} \cdot \nabla C_j = 0 \qquad \mathbf{V} \cdot \mathbf{n} > 0 \text{ on } B_V \tag{20a}$$

$$j = 1, 2, \cdots, N_a$$

$$\mathbf{n} \cdot (VC_j - \theta \mathbf{D} \cdot \nabla C_j) = q_{jV} \qquad \mathbf{V} \cdot \mathbf{n} < 0 \text{ on } B_V \tag{20b}$$

$$j = 1, 2, \cdots, N_a$$

where $\mathbf{n}$ is an outward unit vector normal to the boundary, B_V is a variable boundary segment, and q_{jV} is the variable boundary material flux.

NUMERICAL APPROXIMATION

The solution of the system of (15) and (2)–(13) was coded in HYDROGEOCHEM [*Yeh and Tripathi*, 1990] as follows. For every time step, first, N_s W_j values and N_{eq} are obtained by solving (2) and (3) subject to initial conditions (17) and (18). Second, N_a T_j values are obtained one by one by solving (15) subject to initial and boundary conditions as specified by (16), (19), and (20) assuming S_j and P_j values are known before the iteration. Third, (4)–(13) are solved for C_j, S_j, P_j, c_j, s_j, x_i, y_i, z_i, and p_i. The second and third steps are repeated until convergent solutions are obtained. This completes a one-time step computation.

The finite-element algorithm used in FEMWASTE [*Yeh and Ward*, 1981] was employed for the hydrologic transport simulation in the second step computation. Depending on the type of weighting functions (Galerkin or upstream weighting), the methods of time marching (Crank-Nicolson, backward difference, or mid difference), and the treatment of mass matrix (lumping or no lumping), a total of 12 optional finite-element numerical schemes were used in the hydrologic transport module to achieve stable and convergent solutions for as wide a range of problems as possible. Both direct solution and iteration techniques are included in HYDROGEOCHEM [*Yeh and Tripathi*, 1990] for computational flexibility and efficiency. The hybrid Newton-Raphson and modified bisection methods used in the development of EQMOD (G.-T. Yeh et al., manuscript in preparation) were adapted for chemical equilibrium simulation in the third step calculation. In the hybrid approach, one can apply either the modified bisection method or the Newton-Raphson method to any of the N_a component equations given in (21) to be described below. In the following, we will examine in some detail how the chemical equilibrium model is solved numerically. We will first describe how the chemical equilibrium system is simplified. Then we will state how the precipitation-dissolution, adsorption, ion exchange, redox, and acid-base reactions are treated.

Reduction of Chemical Model Equations

Substituting (10) and (11) into (7), one obtains

$$T_j = c_j + \sum_{i=1}^{M_x} a_{ij}^x \left(\alpha_i^x \prod_{k=1}^{N_a} c_k^{a_{ik}^z} \right) + \sum_{i=1}^{M_y} a_{ij}^y \cdot \left[\alpha_i^y \left(\prod_{k=1}^{N_a} c_k^{a_{ik}^y} \right) \left(\prod_{k=1}^{N_s} s_k^{b_{ik}^y} \right) \right] + \sum_{i=1}^{M_z} a_{ij}^z z_i + \sum_{i=1}^{M_p} a_{ij}^p p_i \quad (21)$$

$$j = 1, 2, \cdots, N_a$$

Substituting (11) into (8), one obtains N_s equations relating W_j to the component species concentrations c_j and s_j as follows:

$$W_j = s_j + \sum_{i=1}^{M_y} b_{ij}^y \left[\alpha_i^y \left(\prod_{k=1}^{N_a} c_k^{a_{ik}^y} \right) \left(\prod_{k=1}^{N_s} s_k^{b_{ik}^y} \right) \right] \quad (22)$$

$$j = 1, 2, \cdots, N_s$$

Equations (21) and (22) along with M_z equations given by (9) and (12) and M_p equations given by (13) form four sets of master equations for four sets of master variables, N_a c_j, N_s s_j, M_z z_i, and M_p p_i. Equations (10), (11), (4), (5), and (6) form five sets of secondary equations for five sets of secondary variables, M_x x_i, M_y y_i, N_a C_j, N_a S_j, and N_a P_j, respectively. It should be emphasized that the four sets of master equations cannot be solved independently of the five sets of secondary equations because the activity coefficient for the proton and the modified equilibrium constants for all species that are present in the four sets of master equations are functions of the secondary variables x_i. Thus in the chemical submodel, these two subsystems must be solved iteratively. The iteration is carried out as follows. First, the ionic strength and the activity coefficients are computed using one of the activity coefficient models [*Davies*, 1962; *Truesdell and Jones*, 1974] based on the values of c_j and x_i from the previous iteration. Second, the modified equilibrium constants are computed using (10*b*), (11*b*), (12*b*), and (13*b*). Third, (21), (22), (9) and (12), and (13) are solved simultaneously for c_j, s_j, z_i, and p_i, respectively. Fourth, (10*a*) and (11*a*) are used to compute x_i and y_i based on newly obtained c_j and s_j and previously obtained modified equilibrium constants. Steps 1 through 4 are repeated until convergent solutions are obtained. Finally, (4)–(6) are used to compute N_a C_j, N_a S_j, and N_a P_j, respectively. These complete the chemical module calculation.

Treatment of Precipitation-Dissolution

In solving the master equations in the chemical submodel, we have assumed that the number of minerals is known a priori. In reality, the number of minerals is not known and must be calculated as part of the solution. An iterative process is used to determine the number of minerals. First, we assume that the number of minerals is known. Second, we solve the chemical equilibrium problem as outlined in steps 1 through 4 in the preceding subsection. Third, after the chemical equilibrium problem is solved with the assumed number of minerals, we check concentrations of all assumed minerals. If the concentration of any mineral is less than zero, then that mineral is forced to dissolve. In the meantime, we also check the solubility product of all potential minerals in the thermodynamic data base. If any potential mineral is supersaturated, this mineral is allowed to precipitate as long as the phase rule is not violated. These three steps are repeated until no change in mineral dissolution or precipitation occurs.

For an assumed number of minerals, precipitation-dissolution can be dealt with by two different approaches. The first is to consider the concentrations of all precipitated species as independent unknowns in addition to the component species concentrations. Thus the master variables will include N_a c_k, N_s s_k, M_z z_i, and M_p p_i. This approach has been used in several geochemical equilibrium models such as EQ3/EQ6 [*Wolery*, 1979] and PHREEQE [*Parkhurst et al.*, 1980], and some multispecies transport models such as THCC [*Carnahan*, 1986]. The second approach is to substitute (13) into (21), (22), (9), and (12) to eliminate M_p (out of N_a) c_k and M_p p_i. Thus the basic master variables will include ($N_a - M_p$) c_k, N_s s_k, and M_z z_i, and the reduced sets of governing equations would be ($N_a - M_p$) of the N_a equations in (21), (22), (9), and (12). The detailed procedure of substituting (13) into (22) and the subsequent reduction of the number of equations can be found in MINEQL [*Westall et al.*, 1976, pp. 56–63]. Using the first approach, one can modify the code to treat mixed chemical equilibrium and chemical kinetics with ease. For simplicity, this paper uses the first approach to treat precipitation-dissolution reactions.

Treatment of Adsorption

The adsorption reactions can be dealt with as in the cases of aqueous complexation since (10) and (11) are similar in form. However, if the double-layer theory [*Davis and Leckie*, 1978] is used to model the adsorption process, two additional unknowns, c_0 and c_b, are introduced in the adsorption-reaction equations in (11). These two additional unknowns are defined as

$$c_0 = \exp(-e\psi_0/kT) \quad (23)$$

$$c_b = \exp(-e\psi_b/kT) \quad (24)$$

where k is the Boltzmann constant, T is the absolute temperature, e is the electronic charge, ψ_0 is the electric potential at the surface, and ψ_b is the electric potential at the beta layer. These two additional unknowns can be obtained by assuming that the total charge calculated by summing over the charges of all surface species is equal to the total charge calculated by electrostatic theory. Written mathematically, these two governing equations are

$$C_1(\psi_0 - \psi_b)B - \sigma_0 = 0 \quad (25a)$$

$$\sigma_0 = \sum_{i=1}^{M_y} a_{i0}^y y_i \quad (25b)$$

$$C_1(\psi_b - \psi_0)B + C_2(\psi_b - \psi_d)B - \sigma_b = 0 \quad (26a)$$

$$\sigma_b = \sum_{i=1}^{M_y} a_{ib}^y y_i \quad (26b)$$

where C_1 is the capacitance of the region between the 0 plane and b plane, B is a conversion factor from charge per unit area to moles per unit volume, σ_0 is the charge density in moles per unit volume on the 0 plane a_{i0}^y is the stoichio-

metric coefficient of c_0 in the ith adsorbed species y_i, C_2 is the capacitance of the region between the b plane and d plane, σ_b is the charge density in moles per unit volume on the b plane, and a_{ib}^{y} is the stoichiometric coefficient of c_b in the ith adsorbed species y_i.

Electroneutrality requires that the following relationship must be satisfied,

$$\sigma_0 + \sigma_b + \sigma_d = 0 \tag{27}$$

and the Gouy-Chapman diffuse layer theory yields the following equation,

$$\sigma_d/B = -(8\varepsilon\varepsilon_0 RIT)^{1/2} \sinh (ze\psi_d/2kT) \tag{28}$$

where σ_d is the charge density in moles per unit volume in the diffusive layer d, R is the universal gas constant, ε is the relative dielectric constant, ε_0 is the permittivity of the free space, and z is the valence of the ion. It should be noted that (28) is valid only for the cases of symmetrical electrolyte. The charge potential relationship gives

$$C_2(\psi_d - \psi_b)B = \sigma_d \tag{29}$$

Combining (28) and (29), we relate the unknowns ψ_d to ψ_b implicitly as follows:

$$C_2(\psi_d - \psi_b) = -(8\varepsilon\varepsilon_0 RIT)^{1/2} \sinh (ze\psi_d/2kT) \tag{30}$$

To solve (25) and (26) with the Newton-Raphson method, we need to evaluate σ_0, σ_b, ψ_0, ψ_b, and ψ_d, and their partial derivatives with respect to c_0 and c_b: $\partial\sigma_0/\partial c_0$, $\partial\sigma_0/\partial c_b$, $\partial\sigma_b/\partial c_0$, $\partial\sigma_b/\partial c_b$, $\partial\psi_0/\partial c_0$, $\partial\psi_0/\partial c_b$, $\partial\psi_b/\partial c_0$, $\partial\psi_b/\partial c_b$, $\partial\psi_d/\partial c_0$, and $\partial\psi_d/\partial c_b$. The evaluation of σ_0 and σ_b, and $\partial\sigma_0/\partial c_0$, $\partial\sigma_0/\partial c_b$, $\partial\sigma_b/\partial c_0$, and $\partial\sigma_b/\partial c_b$ can be performed similarly to the evaluation for other aqueous components. The evaluation of ψ_0, ψ_b, and ψ_d, and $\partial\psi_0/\partial c_0$, $\partial\psi_0/\partial c_b$, $\partial\psi_b/\partial c_0$, $\partial\psi_b/\partial c_b$, $\partial\psi_d/\partial c_0$, and $\partial\psi_d/\partial c_b$ requires a little further elaboration. Knowing c_0 and c_b from a previous iteration, we compute ψ_0 and ψ_b by inverting (23) and (24) as

$$\psi_0 = -\frac{kT}{e} \ln (c_0) \tag{31}$$

$$\psi_b = -\frac{kT}{e} \ln (c_b) \tag{32}$$

respectively. Having computed σ_0 and σ_b from (25b) and (26b), respectively, we compute σ_d from (27) and then invert (28) to obtain ψ_d as

$$\psi_d = \frac{2kT}{ze} \sinh^{-1} [-(\sigma_d/B)/(8\varepsilon\varepsilon_0 RIT)^{1/2}] \tag{33}$$

Differentiating (23) with respect to c_0 and c_b, respectively, we obtain

$$\frac{\partial\psi_0}{\partial c_0} = \left(-\frac{kT}{e}\right)\Big/ c_0 \tag{34a}$$

$$\frac{\partial\psi_0}{\partial c_b} = 0 \tag{34b}$$

Similarly, differentiating (24) with respect to c_0 and c_b, respectively, we obtain

$$\frac{\partial\psi_b}{\partial c_0} = 0 \tag{35a}$$

$$\frac{\partial\psi_b}{\partial c_b} = \left(-\frac{kT}{e}\right)\Big/ c_b \tag{35b}$$

Finally, differentiating (30) with respect to c_0 and c_b, respectively, and substituting (35) into the resulting equation, we obtain

$$\frac{\partial\psi_d}{\partial c_0} = 0 \tag{36a}$$

$$\frac{\partial\psi_d}{\partial c_b} = \left[\left(-\frac{kT}{e}\right)\Big/ c_b\right]\Big/\left[1 + \left(\frac{e}{2kT}\right) \cdot (8\varepsilon\varepsilon_0 RIT)^{1/2} \cosh\left(\frac{ze\psi_d}{2kT}\right)\Big/ C_2\right] \tag{36b}$$

Treatment of Ion Exchange

For sorption via ion exchange, (9) and (12) can easily be written explicitly in terms of component species concentration if the ion exchange involves only homovalent exchange. Under such circumstances, the computation of the Jacobian (9) and (12) is relatively easy and can be performed analytically. However, when ion exchanges involve heterovalent exchange, it is very difficult if not impossible to express the concentration of ion-exchanged species in terms of component species concentrations. In other words, the analytical computation of the Jacobian cannot be done easily. Therefore, for purposes of generality, numerical evaluations of the Jacobian involving ion exchange reactions are used in this paper.

Treatment of Oxidation-Reduction

Oxidation-reduction reactions are treated by defining electron activity rather than the concentration of free electrons as a master variable, and making the "operational" electron subject to transport as are other aqueous components. If a chemical element is present at several oxidation states, only one of these can be considered a component and the others must be treated as species described by a half-cell reaction which is analogous to the complexation. For example, if Fe^{2+} and Fe^{3+} are present simultaneously in a system, we may consider Fe^{3+} a component species. Then Fe^{2+} shall be considered a complexed species, which is a product of Fe^{3+} and e^-. A mole of Fe^{2+} is considered to contribute a mole of operational electrons and a mole of Fe^{3+}. The total "operational" electron is obtained by solving the transport equation, (15), with $j = e$. The mole balance equation for the "operational" electron is different from those for other aqueous components in that the first term on the right-hand side of (21) is set to zero and c_e (i.e., set $k = e$ in c_k) in all other terms is interpreted as the activity of the electron rather than the concentration of free electrons.

Although mathematically the "operational electron" can be treated just as other aqueous components, numerically this component requires special attention. Because the electron activity can span over at least 40 orders of magnitude, the solution of the balance equation of the "operational"

electron often renders the Newton-Raphson matrix ill-conditioned when this equation is solved simultaneously with other mole balance equations. To circumvent this difficulty, a split scheme is used in this paper. In this split scheme, the mole balance equation for the "operational" electron is solved for the electronic activity with a modified bisection method [*Forsythe et al.*, 1977] while all other mole balance equations are solved simultaneously with the Newton-Raphson method. This split scheme is very effective, in particular for reducing conditions when the solution often fails to converge without the split scheme.

Treatment of Acid-Base Reactions

Acid-base reactions are treated by defining proton activity as a master variable and making the "excess" proton subject to transport as are other aqueous components. The mole balance equation is defined for the "excess" proton rather than the proton itself. Thus this mole balance equation is different from those for other aqueous components in two respects. First, because the proton activity rather than the proton concentration is the master variable, the first term on the right-hand side of (21) should be written as c_H/γ_H, and c_H (i.e., set $k = H$ in c_k) in all other terms is interpreted as the proton activity rather than the proton concentration, where γ_H is the activity coefficient of the proton ion. Second, because the mole balance is defined based on "excess" proton concentration, if a hydroxide (OH^-) appears in any species, the stoichiometric coefficient of the proton in that species should be set to -1. If n hydroxides appear in any species, the stoichiometric coefficient of the proton in that species should be set to $-n$. On the other hand, if a hydronium (H^+) appears in a species, the stoichiometric coefficient of the proton in that species is 1. If n hydroniums appear in a species, the stoichiometric coefficient of the proton in the species is n. As a result, the only major difference between the proton as an aqueous component and all other regular aqueous components is that the former can have a negative total analytical concentration, but the latter cannot have negative total analytical concentrations. Since the total analytical concentration of the excess proton can be negative, the continuous fraction [*Wigley*, 1977] method is not an appropriate tool for solving for the proton activity. Instead, either the modified bisection method or the Newton-Raphson method is applied to the mole balance equation of the excess proton.

EXAMPLE PROBLEMS FOR TESTING AND DEMONSTRATION

During the course of development and modification, the HYDROGEOCHEM model was used to solve several dozen problems of varying complexity. It continues to be used to model hypothetical and real systems on laboratory and field scales. The example problems are selected to demonstrate some of the capabilities and features of HYDROGEOCHEM. A companion paper, in preparation, will discuss application of the model to a variety of problems in environmental and earth sciences including uranium mill tailings, acid mine drainage, mixed-waste disposal, genesis of sedimentary uranium ores and hydrogeochemical mineral exploration.

A series of four example problems are presented. Problem 1 serves to verify the hydrologic transport module of HYDROGEOCHEM; additionally, it illustrates the ease with which the explicit form of the transport equation, (14), can encounter negative concentrations. Problems 2 through 4 illustrate the capabilities of the coupled model by displaying the interplay of hydrologic transport and chemical interactions. Each example includes a description of the problem and a discussion of the results and their significance. The list of aqueous and adsorbed species and minerals considered for each problem is provided in Tables 2–4.

The selection of chemical species and thermodynamic data is critical to successful application of geochemical and hydrogeochemical models to natural systems [*Tripathi*, 1983]. Since the purpose of this paper is to demonstrate the capabilities of the HYDROGEOCHEM model and to demonstrate the outcome of interactions among transport and chemical processes, no attempt was made at critical selection of thermodynamic data.

Only one problem was used to test the transport module of HYDROGEOCHEM since it is adapted from FEMWASTE [*Yeh and Ward*, 1981], which has been extensively tested. The chemical module of HYDROGEOCHEM, EQMOD, is new; it was extensively tested and the results were verified for six chemical processes of aqueous complexation, precipitation-dissolution, adsorption-desorption, ion exchange, oxidation-reduction, and acid-base reactions as well as any combination of these six processes [*Yeh and Tripathi*, 1990].

Problem 1: Test of Hydrologic Transport

The problem deals with transport in a one-dimensional column 0.5 dm long; the flow velocity from the bottom to top is 10^{-2} dm/h, the effective porosity was 0.3, the bulk density 1.2 g/cm^3, and the dispersivity was 2×10^{-3} dm. The transport involves two chemical components. The initial conditions are that total analytical concentrations are 0.1 M for both chemical components. The boundary conditions are as follows: at $z = 0.0$ dm, total analytical concentrations are specified at 1.0 M; at $z = 0.5$ dm, variable boundary conditions with zero gradient fluxes are specified for both components.

To mimic the hydrologic transport without interaction between two chemical components, we assume that each chemical component has two species: one a free species and the other an adsorbed species. The ratios of the adsorbed species to the free species are assumed to be 1/9 and 9, respectively, for chemical components 1 and 2. In other words, there was a 10% and 90% adsorption, respectively, for chemicals 1 and 2. To put it in terms of geochemical equilibrium constants, the two thermodynamic equilibrium constants for the two adsorbed species are 1/9 and 9, respectively. In order to deal with the situation of no interaction between components, the adsorbent component is not considered, i.e., the adsorbing site is not a constraint for the equilibrium between free species and adsorbed species for each component.

For numerical simulation, the column is discretized by 1 × 20 elements of size 0.025 dm × 0.025 dm, which results in 42 nodes. The simulation was conducted for three time steps only since the purpose of this simulation is simply to verify the hydrologic module. The time step size was 0.5 hours.

Table 1 lists the total analytical concentrations at various points after three time step simulations for the cases of 10%

TABLE 1. Comparison of Explicit and Implicit Iterations

	10% Dissolved			90% Dissolved		
x	Explicit	Implicit	One-Step	Explicit	Implicit	One-Step
0.000	1.0000	1.0000	1.0000	1.0000	1.0000	1.0000
0.025	0.2680	0.2680	0.2680	0.7673	0.7850	0.7850
0.050	0.1219	0.1219	0.1219	0.6368	0.5437	0.5437
0.075	0.1024	0.1024	0.1024	0.1015	0.3595	0.3595
0.100	0.1002	0.1002	0.1002	0.4020	0.2415	0.2415
0.125	0.1000	0.1000	0.1000	−0.0405	0.1734	0.1734
0.150	0.1000	0.1000	0.1000	0.4135	0.1367	0.1367
0.175	0.1000	0.1000	0.1000	−0.0390	0.1178	0.1178
0.200	0.1000	0.1000	0.1000	0.2631	0.1085	0.1085
0.225	0.1000	0.1000	0.1000	−0.0648	0.1039	0.1039
0.250	0.1000	0.1000	0.1000	0.2788	0.1018	0.1018
0.275	0.1000	0.1000	0.1000	−0.0155	0.1008	0.1008
0.300	0.1000	0.1000	0.1000	0.2071	0.1004	0.1004
0.325	0.1000	0.1000	0.1000	−0.0242	0.1002	0.1002
0.350	0.1000	0.1000	0.1000	0.2461	0.1001	0.1001
0.375	0.1000	0.1000	0.1000	−0.0327	0.1000	0.1000
0.400	0.1000	0.1000	0.1000	0.2013	0.1000	0.1000
0.425	0.1000	0.1000	0.1000	0.0201	0.1000	0.1000
0.450	0.1000	0.1000	0.1000	0.2351	0.1000	0.1000
0.475	0.1000	0.1000	0.0100	−0.0602	0.1000	0.1000
0.500	0.1000	0.1000	0.1000	0.2880	0.1000	0.1000

and 90% dissolved using explicit and implicit iterations. Included also in Table 1 is the result using a one-step direct solution method, i.e., without having to iterate between the hydrologic transport module and the geochemical equilibrium module. It is seen that the implicit iteration solution yields identical results as the one-step direction solution method for both cases. Thus the implicit iteration algorithm is verified. On the other hand, while the explicit iteration solution yields identical solution to the one-step solution method for the case of 10% dissolved, it produces a noncon-

TABLE 2. Chemical Species for Example 2

		Stoichiometry					
Species	log K	Component	Value	Component	Value	Component	Value
		Aqueous Species					
H^+	0.00	H	1.0				
CO_3	0.00	CO_3	1.0				
Ca^{2+}	0.00	Ca	1.0				
Mg^{2+}	0.00	Mg	1.0				
SO_4^{2-}	0.00	SO_4	1.0				
OH^-	−13.99	H	−1.0				
$CaCO_3$	3.22	Ca	1.0	CO_3	1.0		
$CaHCO_3^+$	11.43	Ca	1.0	CO_3	1.0	H	1.0
$CaSO_4$	2.31	Ca	1.0	SO_4	1.0		
$CaOH^+$	−12.85	Ca	1.0	H	−1.0		
$MgCO_3$	2.98	CO_3	1.0	Mg	1.0		
$MgHCO_3^+$	11.40	CO_3	1.0	H	1.0	Mg	1.0
$MgSO_4$	2.25	SO_4	1.0	Mg	1.0		
$MgOH^+$	−11.44	H	−1.0	Mg	1.0		
HCO_3^-	10.32	CO_3	1.0	H	1.0		
H_2CO_3	16.67	CO_3	1.0	H	2.0		
HSO_4^-	1.99	SO_4	1.0	H	1.0		
		Minerals Allowed to Precipitate					
Calcite	8.48	Ca	1.0	CO_3	1.0		
$MgCO_3$	8.20	Mg	1.0	CO_3	1.0		
Gypsum	4.62	Ca	1.0	SO_4	1.0		
Calcium hydroxide	−21.90	Ca	1.0	H	−2.0		
$Mg_2(OH)_2CO_3$	−9.65	CO_3	1.0	H	−2.0	Mg	2.0
$Mg_5(OH)_2(CO_3)_4$	9.72	CO_3	4.0	H	−2.0	Mg	5.0
$Mg(OH)_2$	−16.80	H	−2.0	Mg	1.0		
$MgSO_4$	2.14	SO_4	1.0	Mg	1.0		
		Minerals Not Allowed to Precipitate					
Dolomite	17.02	Ca	1.0	CO_3	2.0	Mg	1.0

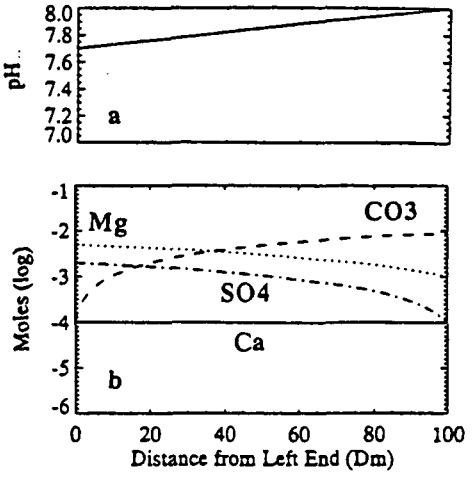

Fig. 1. (*a*) The *p*H distribution in the column. (*b*) Initial distribution of total calcium, magnesium, carbonate and sulfate in the column.

vergent oscillating solution for the case of 90% dissolved as speculated earlier in this paper. This confirms our intuitive speculation that the explicit iteration can easily tumble into negative concentrations.

Problem 2: Simulation of Transport With Complexation and Precipitation in a One-Dimensional Column

The problem is designed to simulate chemical concentration patterns evolving from complex changes in chemical compositions resulting from fluid flow, time-dependent boundary conditions, and precipitation and dissolution of minerals. Additional objectives were to simulate the formation of multiple precipitation-dissolution fronts, and to demonstrate the need to iterate between hydrologic and chemical modules at each time step. The latter objective was defined in view of some previous work in the published literature wherein the chemical module was called only once at each time step [*Liu and Narasimhan*, 1989*a*, *b*].

To permit unambiguous interpretation of model response, the number of components and the minerals allowed to precipitate was kept small. A one-dimensional column was discretized into 100 elements of size 1 dm × 1 dm. The density of the porous medium was 1.2 g/cm^3. The fluid entered from the right end of the column at a velocity of 0.5 dm/day. The porosity of the medium was 0.3 and the dispersivity was 5 dm. The simulation was conducted for 250 days with a time step of 0.5 days. Five chemical components, namely, calcium, magnesium, carbonate, sulfate and hydronium, 12 aqueous species, and eight possible minerals were considered (see Table 2). The precipitation of dolomite was not considered since it does not readily precipitate in

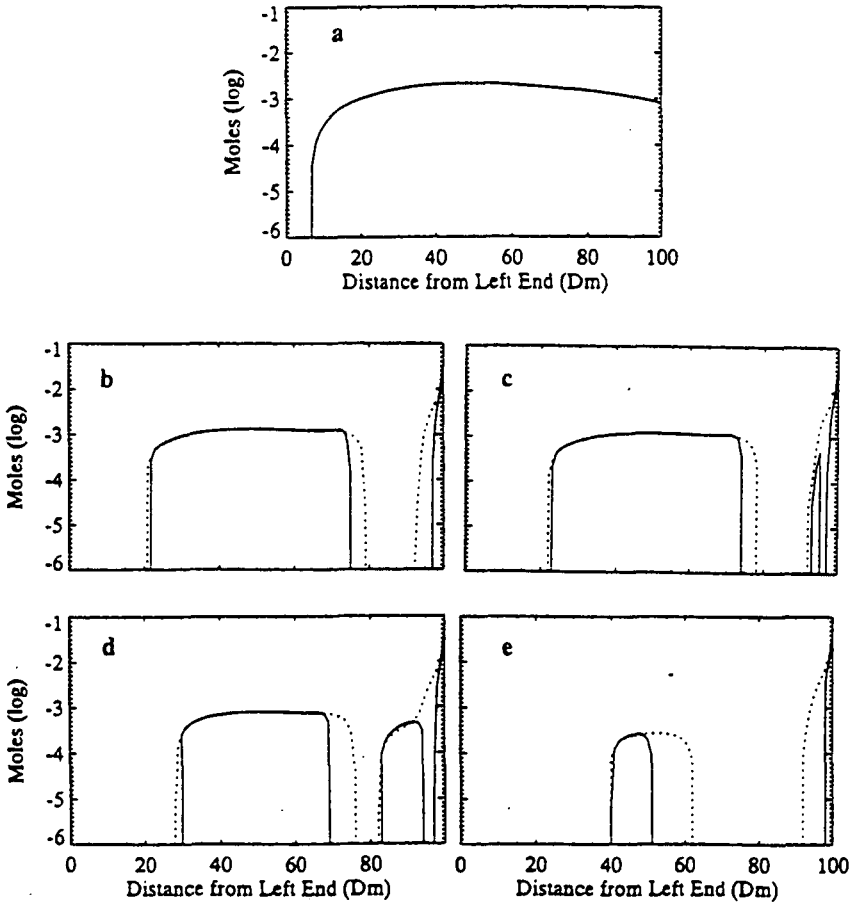

Fig. 2. Distribution of magnesium carbonate precipitation in the column at various times: (*a*) 0, (*b*) 130, (*c*) 140, (*d*) 190, and (*e*) 250 days. The dotted lines show the corresponding results when the number of iterations between the hydrologic and the chemical modules is limited to one.

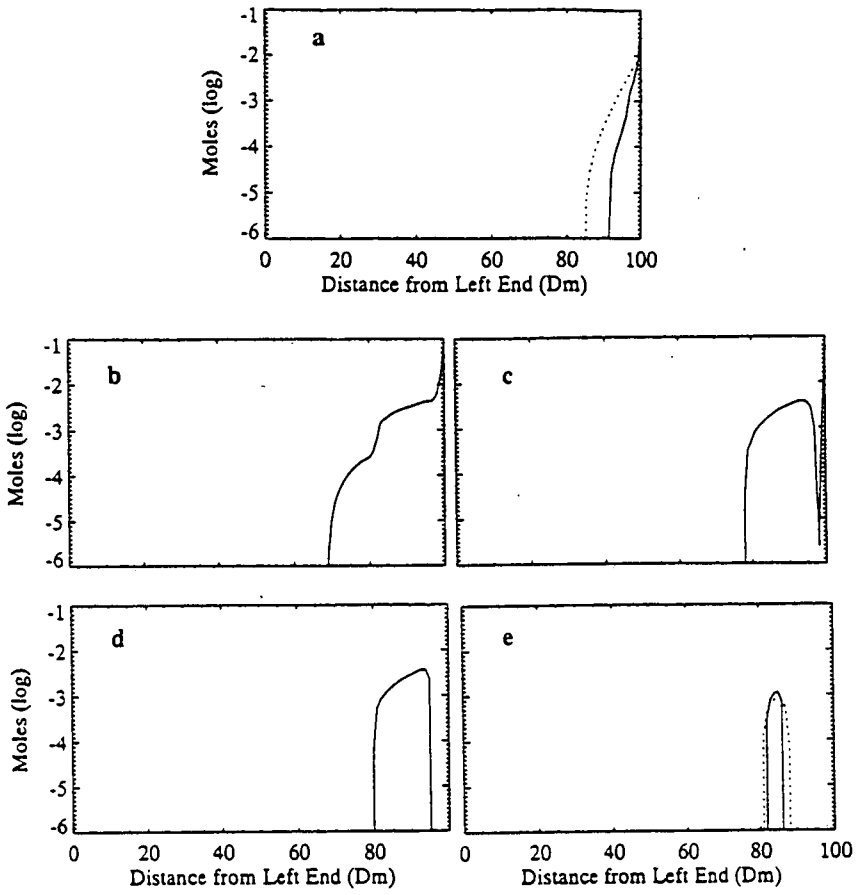

Fig. 3. Distribution of calcium carbonate precipitation in the column at various times: (*a*) 3, (*b*) 15, (*c*) 80, (*d*) 130, and (*e*) 180 days. The dotted lines show the corresponding results when the number of iterations between the hydrologic and the chemical modules is limited to one.

low-ionic strength solutions. The initial concentration of chemical components in the column was defined to promote precipitation of calcium carbonate and magnesium carbonate. The *p*H was fixed throughout the system (Figure 1*a*) between 7.7 and 8.0. The initial calcium concentration was fixed at 10^{-4} M. The initial magnesium concentration decreased from 5×10^{-3} M at the left end of the column to 10^{-3} M at the right end of the column; similarly, the initial sulfate concentration decreased from 2×10^{-3} M to 10^{-4} M from left to right (Figure 1*b*). Contrary to the trend in sulfate and magnesium, the carbonate concentration increased from left to right as shown in Figure 1.

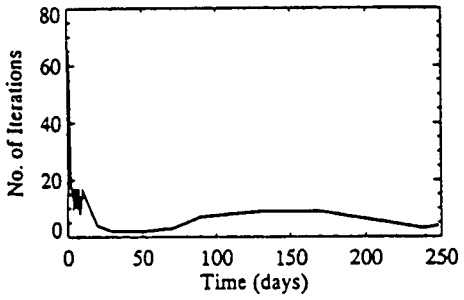

Fig. 4. The number of iterations between the hydrologic and the chemical modules required for convergence at each time step of HYDROGEOCHEM.

The boundary conditions for chemicals entering the right end of the column were set at 2×10^{-3}M, 10^{-3} M, and 2×10^{-3} M for carbonate, magnesium and sulfate, respectively. The boundary condition for calcium was set at 10^{-4} M for all times with the exception that from day 1 to 9.5 days, its concentration increased 90-fold to 9×10^{-3} M. The pulse in calcium concentration was introduced to induce changes in the degree of supersaturation of carbonate minerals with space and time as the pulse traveled within the column. The behavior of magnesium and calcium precipitation in the column is analyzed. In all figures for this example, normal HYDROGEOCHEM results are shown as solid lines, while those with the number of interhydrogeochemical iterations limited to one are shown as dotted lines.

At time 0 magnesium carbonate precipitation occurred in most of the column (Figure 2*a*). By 130 days, the precipitation zone throughout most of the column at time 0 decreased in width, and a narrow precipitation peak developed near the fluid entrance to the column (Figure 2*b*). The dissolution of magnesium carbonate near the right end of the column occurred because of competition for carbonate from calcium as shown in Figure 3*d*. At 140 days, two separate peaks of magnesium carbonate precipitate developed near the right end of the column; at this point five dissolution-precipitation fronts existed in the column. At 190 days, the middle peak broadened (Figure 2*d*); however, as the carbonate concentration continued to evolve, by 250 days, the middle peak

TABLE 3. Chemical Species for Example 3

Species	log K	Stoichiometry					
		Component	Value	Component	Value	Component	Value
			Aqueous Species				
H^+	0.00	H	1.0				
UO_2^{2+}	0.00	UO_2	1.0				
NpO_2^+	0.00	NpO_2	1.0				
CO_3^{2-}	0.00	CO_3	1.0				
SO_4^{2-}	0.00	SO_4	1.0				
OH^-	−13.99	H	−1.0				
$CaCO_3$	3.22	Ca	1.0	CO_3	1.0		
$CaHCO_3^+$	11.43	Ca	1.0	CO_3	1.0	H	1.0
$CaSO_4$	2.31	Ca	1.0	SO_4	1.0		
$CaOH^+$	−12.85	Ca	1.0	H	−1.0		
UO_2OH^+	−5.30	UO_2	1.0	H	−1.0		
$(UO_2)_2(OH)_2^{2+}$	−5.68	UO_2	2.0	H	−2.0		
$(UO_2)_3(OH)_4^{2+}$	−11.88	UO_2	3.0	H	−4.0		
$(UO_2)_3(OH)_5^+$	−15.82	UO_2	3.0	H	−5.0		
$(UO_2)_4(OH)_7^+$	−21.90	UO_2	4.0	H	−7.0		
$(UO_2)_3(OH)_7^-$	−28.34	UO_2	3.0	H	−7.0		
UO_2CO_3	9.65	CO_3	1.0	UO_2	1.0		
$UO_2(CO_3)_2^{2-}$	17.08	CO_3	2.0	UO_2	1.0		
$UO_2(CO_3)_3^{4-}$	21.70	CO_3	3.0	UO_2	1.0		
$(UO_2)_2(OH)_3CO_3^-$	−1.18	CO_3	1.0	UO_2	2.0	H	−3.0
UO_2SO_4	2.95	UO_2	1.0	SO_4	1.0		
$UO_2(SO_4)_2^{2-}$	4.00	UO_2	1.0	SO_4	2.0		
HCO_3^-	10.32	CO_3	1.0	H	1.0		
H_2CO_3	16.67	CO_3	1.0	H	2.0		
HSO_4^-	1.99	SO_4	1.0	H	1.0		
NpO_2OH	−8.85	NpO_2	1.0	H	−1.0		
NpO_2CO_3	5.60	CO_3	1.0	NpO_2	1.0		
$NpO_2(CO_3)_2^{3-}$	7.75	CO_3	2.0	NpO_2	1.0		
			Surface Species				
SOH	0.00	SOH	1.0				
SO^-	−10.30	SOH	1.0	H	−1.0		
SOH_2^+	5.40	SOH	1.0	H	1.0		
$SO^-UO_2OH^\bullet$	−7.10	SOH	1.0	UO_2	1.0	H	−2.0
$SOH_2^+(UO_2)_3(OH)_7^-$	−31.00	SOH	1.0	UO_2	3.0	H	−8.0
$SOHN_pO_2OH$	−3.50	SOH	1.0	NpO_2	1.0	H	−1.0
			Minerals				
Rutherfordine	14.11	CO_3	1.0	UO_2	1.0		
Calcite	8.48	Ca	1.0	CO_3	1.0		
Gypsum	4.62	Ca	1.0	SO_4	1.0		
Calcium hydroxide	−21.90	Ca	1.0	H	−2.0		
Uranyl hydroxide	−5.55	UO_2	1.0	H	−2.0		
Schoepite	−5.40	UO_2	1.0	H	−2.0		

entirely vanished, and the precipitation zone in the center of the column narrowed considerably (Figure 2*e*). The complex precipitation-dissolution interfaces were defined automatically by HYDROGEOCHEM in response to changes in chemical composition of the system. Unlike certain solute transport models [*Rubin*, 1983], in HYDROGEOCHEM there is no need to know the number of interfaces a priori, and a large number of interfaces does not cause difficulties.

The precipitation dynamics of calcium carbonate in the column were considerably different from those of magnesium carbonate as shown in Figures 3*a*–3*d*. Initially, there was precipitation near the right end of the column; it broadened considerably by day 15 (Figure 3*b*). With time, the width of precipitation decreased (Figures 3*a*–3*c*), and by 240 days it dissolved completely.

Many transport models [*Walsh et al.*, 1984; *Liu and Narasimhan*, 1989*a*, *b*] that deal with solute transport in

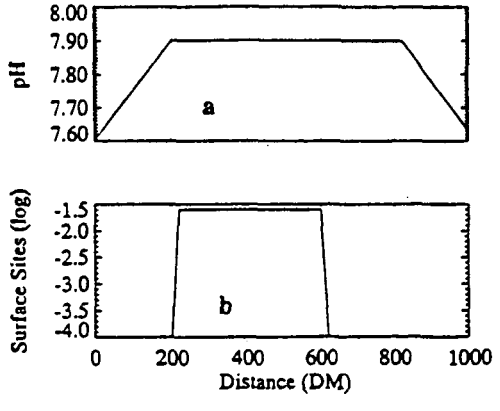

Fig. 5. (*a*) The *p*H distribution in the column. (*b*) Distribution of total surface sites (of goethite) in the column. The *p*H and surface sites are invariant with time.

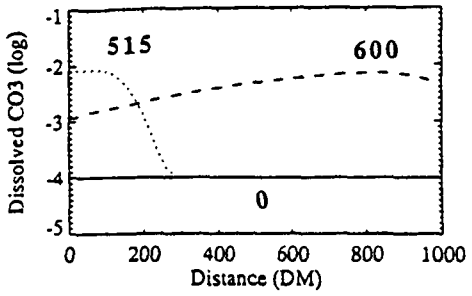

Fig. 6. Distribution of total dissolved carbonate in the column at various times: 0, 515, and 600 days.

reactive systems perform hydrologic and chemical computations in separate modules in the same manner as HYDROGEOCHEM. But unlike HYDROGEOCHEM, some of these models do not iterate between the hydrologic and the chemical submodels; they perform the chemical computations only once at each node at each time step [*Liu and Narasimhan*, 1989*a*, *b*]. In HYDROGEOCHEM, many iterations between the hydrologic and chemical submodels are sometimes required for convergence in the transport equations. The number of such iterations required for this example varied from 64 to two (Figure 4). The effect of limiting the number of such iterations to one on the results produced by HYDROGEOCHEM was evaluated; the dotted lines in Figures 2 and 3 show these simulation results. The dotted lines in Figures 2*b*–2*e* show that if the number of iterations between the hydrologic and chemical submodels is limited to one, HYDROGEOCHEM fails to correctly calculate the spatial distribution of magnesium carbonate precipitation. As high as 10^{-2} M magnesium carbonate precipitate is shown where it should have been 0; often two separate precipitation peaks were combined into one when iterations between the hydrologic and chemical model were prevented. Similarly, Figures 3*a* and 3*e* show that the amount of precipitated calcium carbonate was also overestimated.

The results illustrate that HYDROGEOCHEM can be used to simulate multifront dissolution-precipitation in highly nonlinear systems, and indicate that iteration between the hydrologic and chemical submodels is critical to accurate calculations.

Problem 3: Simulation of Transport, in One Dimension, of Uranium (VI) and Neptunium (V) in Response to Complexation With Carbonate and Adsorption-Desorption Onto Goethite

This example considers the transport and chemical interactions in a one-dimensional column. The fundamental objective in designing the example was to examine the likelihood of achieving greater concentrations of a solute in the interior of the column than in the incoming solution, in response to chemical processes, chiefly complexation and adsorption-desorption, and fluid flow. Achieving such a condition would mean that the concentration of a contaminant could be higher at a point away from the source than near the source. Also, this condition would be totally contrary to the predictions made by single-value-K_d-based transport models which always predict monotonically decreasing contaminant concentrations away from the contaminant source.

A one-dimensional column discretized into 50 elements of size 20 dm × 20 dm was used. The fluid entered at the left end at a velocity of 3 dm/day. The porosity of the medium was 0.3 and the bulk density was 1.2 g/cm^3. The dispersivity was 1 dm. The simulation was conducted for 600 days with a time step of 1 day. Seven chemical components, namely, calcium, carbonate, sulfate, uranium (VI), neptunium (V), hydronium (H^+) and SOH (adsorption sites on mineral surfaces) were considered. The components formed 23 aqueous complexes, five surface complexes (adsorbed species) and six possible minerals (see Table 3). The precipitation of minerals was not allowed so that partitioning of solutes between the solid and the solution phases was controlled

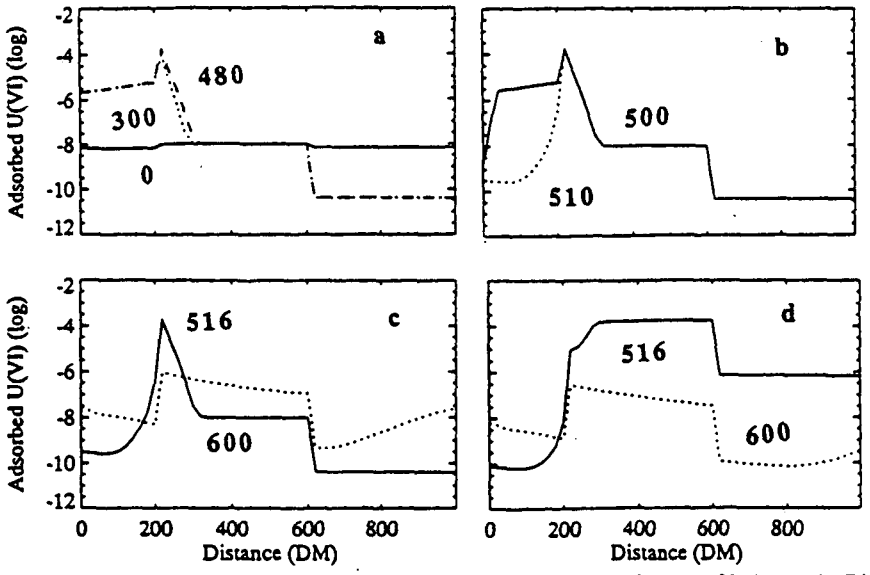

Fig. 7. (*a*) Distribution of adsorbed uranium in the column at times 0, 300, and 480 days. (*b*) Distribution of adsorbed uranium in the column at times 500 and 510 days; (*c*) Distribution of adsorbed uranium in the column at times 516 and 600 days. (*d*) Variation of calculated log (K_d) in the column at times 516 and 600 days.

13

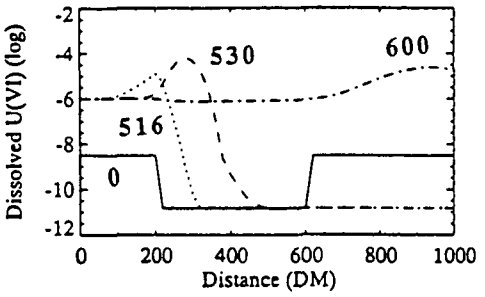

Fig. 8. Evolution of the peak in dissolved uranium concentration in the column at 0, 516, 530, and 600 days, respectively.

solely by adsorption and desorption. The electrostatic interactions were not considered in adsorption computations for simplification. The initial pH in the column was fixed within a narrow range between 7.6 and 7.9 (Figure 5*a*). The initial calcium concentration was set to 10^{-4} M. The initial concentration of carbonate and sulfate, ligands capable of complexing with uranium and neptunium, was kept low, 10^{-4} M, to minimize complexation. A zone rich in adsorption sites (represented by goethite, a ferric oxyhydroxide) was created at a distance of 200 to 600 dm from the left end of the column by specifying the concentration of surface sites (available to 1 L of solution) of 2.5×10^{-2} M; the surface site concentration elsewhere in the column was 10^{-4} M, or 250 times less (Figure 5*b*). The higher concentration of surface sites was chosen to facilitate adsorption of uranium and neptunium in the region and is consistent with iron-rich bands in many natural sediments and rocks. The initial concentration of uranium (VI) and neptunium (V) in the column was 10^{-8} M and 10^{-16} M respectively.

The boundary condition (composition of the groundwater entering the left end of the column) was set differently for different components. The calcium concentration was held constant at 10^{-3} M throughout the simulation. Similarly, the sulfate concentration was set to 10^{-4} M, the same low value as within the column. The boundary concentrations of uranium (VI) and neptunium (V) were set at 10^{-6} M and 2.5×10^{-10} M respectively. The pH of incoming groundwater was set to 7.6. The concentration of carbonate in the incoming groundwater was set to vary with time. For the first 498 days, the carbonate concentration was set to the same low value of 10^{-4} M as within the column to facilitate adsorption of uranium and neptunium. However, for a short period between 498 and 502 days, the carbonate concentration was increased 100 times to 10^{-2} M; from 502 to 599 days the carbonate concentration decreased linearly from 10^{-2} M to 10^{-3} M. The increase in carbonate concentration was introduced to effect desorption of uranium and neptunium from goethite due to increased carbonate complexation. Figure 6 shows that the peak in carbonate concentration arrives in the adsorbent-rich zone in the column at about 515 days. The carbonate concentration profile was pivotal in controlling the adsorption dynamics in the column. Only the behavior of uranium adsorption-desorption is described for brevity.

Figure 7*a* shows the development of a uranium-rich zone due to adsorption. It should be noted that even though less than 2% of the surface sites are occupied by uranyl ions, the concentration of uranium on the surface at 300 to 480 days is more than 20,000 times that in the incoming groundwater. As the carbonate pulse released at 498 days reaches the adsorbed uranium, carbonate complexation causes desorption (Figure 7*b*); the desorption of uranium continues as the carbonate pulse arrives in the adsorbent-rich zone (Figure 7*c*). The profound changes in the extent of uranium adsorption are reflected in the more than 6 orders of magnitude variation in the calculated K_d for uranium with time and space (Figure 7*d*). The increase in uranium adsorption for the first 498 days and then a decrease are reflected in the strong variation in the concentration of dissolved uranium in the column as shown in Figure 8. The figure shows that at time 0, the concentration of dissolved uranium is uniformly less, due to adsorption, than the uranium concentration in the incoming water. However, due to carbonate-induced desorption of uranium, a pulse of uranium concentration is created in the groundwater that is 6800 times the uranium concentration in the incoming water. Due to dispersion the pulse peak is gradually reduced; however, even at 600 days, the dissolved uranium concentration at the downstream end is 2000 times that in the incoming groundwater. The dramatic results would have never been possible without explicit consideration of adsorption, desorption and complexation processes; a K_d-based model would not produce such results. The large peak in dissolved uranium is produced due to the assumption of instantaneous desorption caused by a 100-fold increase in carbonate concentration. The kinetics of adsorption and desorption of uranyl, as known to date, suggest that in natural systems, kinetic factors may reduce the peak height much in the same way as dispersion does. However, despite the slow kinetics, elevated concentrations of dissolved uranium would still develop.

The results of this simulation show the importance of accounting for chemical processes; they also show that unlike the predictions of the single-value-K_d-based models, the aqueous concentration of a contaminant can be greater at a point farther away from its source than at one near the source. The result is especially significant in designing field surveys for detecting and defining the extent of the contaminant plume.

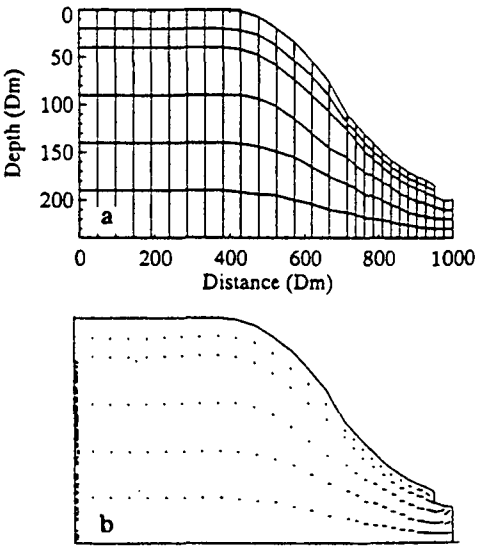

Fig. 9. (*a*) Finite element mesh for the uranium mill tailings problem. (*b*) Steady state flow field through the cross section.

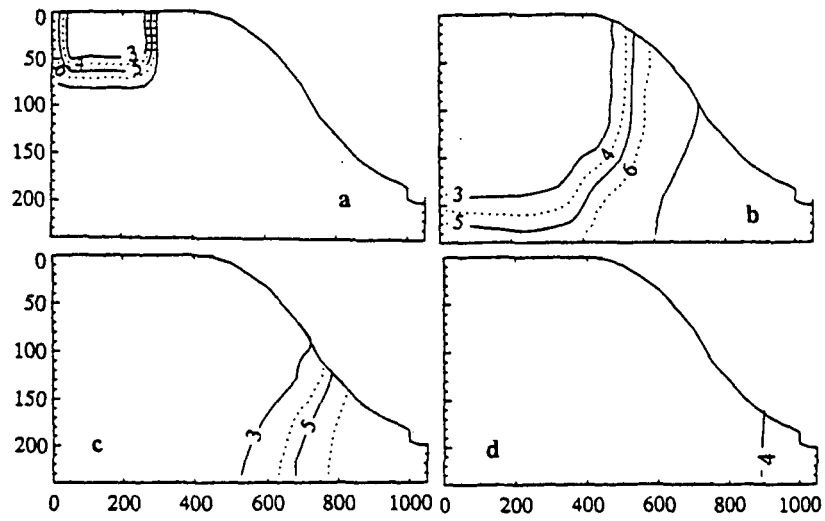

Fig. 10. Distribution of pH in the system at various times: (*a*) 0, (*b*) 3000, (*c*) 6000, and (*d*) 7920 days.

Problem 4: Simulation of Release and Transport, in Two Dimensions, of Acidity (H^+), Uranium (VI), and Molybdate and the Changes in Major Element Mineralogy From a Uranium Mill Tailings Pile

This example considers a simplified hypothetical problem of the release of trace metals and acidity from an acidic uranium mill tailings pile. The problem was selected to demonstrate the ability of HYDROGEOCHEM to predict some of the well-known features associated with acidic mill tailings, e.g., the replacement of calcite by gypsum due to release of acidity and sulfate from the tailings pile. It was also designed to examine the impact of precipitation-dissolution reactions on retardation of toxic metals released from waste sites.

A two-dimensional vertical cross section is considered. The region is discretized with 152 elements and 192 nodes (Figure 9*a*). The vertical left edge (24 m) is a no-flow boundary; the horizontal bottom (100 m) is also an impermeable no-flow boundary. The sloping region on the top right has a variable boundary with either zero ponding depth or a net rainfall rate of 0.0139 dm/day. The horizontal region of the top boundary is a Cauchy boundary with an infiltration rate of 0.139 dm/day. The five nodes on the vertical right side and the two nodes on "river" bottom are specified as known-head conditions (Dirichlet boundary condition). The total head for the five vertical nodes was given as 39 dm. The total head on the left and right nodes of the river bottom is specified as 44 dm and 40 dm, respectively. The steady state flow was calculated with the HYDROGEOFLOW program (a simplified version of FEMWATER [*Yeh*, 1987]) and the flow field is given in Figure 9*b*.

The chemical problem considers seven components, namely, calcium, carbonate, uranium (VI), sulfate, phosphate, molybdate and hydronium. A total of 32 aqueous complexes and 12 possible minerals were considered (see Table 4). Redox reactions were not considered as the goal was to simulate acidification and dissolution-precipitation reactions and their impact on migration of trace metals. The redox conditions of some uranium mill tailings sites in the western United States are relatively oxidizing, suggesting

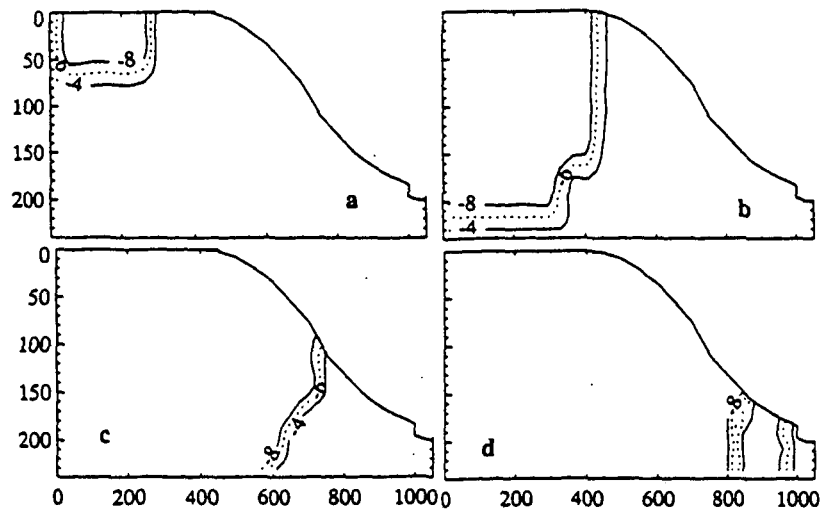

Fig. 11. Distribution of calcite (log moles) in the system at various times: (*a*) 0, (*b*) 1000, (*c*) 4000, and (*d*) 7000 days.

TABLE 4. Chemical Species for Example 4

Species	log K	Stoichiometry					
		Component	Value	Component	Value	Component	Value
			Aqueous Species				
Ca^{2+}	0.00	Ca	1.0				
CO_3^{2-}	0.00	CO_3	1.0				
UO_2^{2+}	0.00	UO_2	1.0				
PO_4^{3-}	0.00	PO_4	1.0				
SO_4^{2-}	0.00	SO_4	1.0				
H^+	0.00	H	1.0				
MoO_4^{2-}	0.00	MoO_4	1.0				
$CaCO_3$	3.22	Ca	1.0	CO_3	1.0		
$CaHCO_3^+$	11.43	Ca	1.0	H	1.0	CO_3	1.0
$CaSO_4$	2.31	Ca	1.0	SO_4	1.0		
CaH_2PO_4	20.96	Ca	1.0	PO_4	1.0	H	2.0
$CaPO_4^-$	6.46	Ca	1.0	PO_4	1.0		
$CaHPO_4$	15.08	Ca	1.0	PO_4	1.0	H	1.0
$CaOH^+$	−12.85	Ca	1.0	H	−1.0		
UO_2OH^+	−5.30	UO_2	1.0	H	−1.0		
$(UO_2)_2(OH)_2^{2+}$	−5.68	UO_2	2.0	H	−2.0		
$(UO_2)_3(OH)_4^{2+}$	−11.88	UO_2	3.0	H	−4.0		
$(UO_2)_3(OH)_5^+$	−15.82	UO_2	3.0	H	−5.0		
$(UO_2)_4(OH)_7^+$	−21.90	UO_2	4.0	H	−7.0		
$(UO_2)_3(OH)_7^-$	−28.34	UO_2	3.0	H	−7.0		
UO_2CO_3	9.65	CO_3	1.0	UO_2	1.0		
$UO_2(CO_3)_2^-$	17.08	CO_3	2.0	UO_2	1.0		
$UO_2(CO_3)_3^{4-}$	21.70	CO_3	3.0	UO_2	1.0		
$(UO_2)_3(OH)_3CO_3^-$	−1.18	CO_3	1.0	UO_2	2.0	H	−3.0
UO_2SO_4	2.95	UO_2	1.0	SO_4	1.0		
$UO_2(SO_4)_2^{2-}$	4.00	UO_2	1.0	SO_4	2.0		
$UO_2H_2PO_4^+$	23.20	UO_2	1.0	PO_4	1.0	H	2.0
$UO_2H_3PO_4^{2+}$	22.90	UO_2	1.0	PO_4	1.0	H	3.0
$UO_2H_4(PO_4)_2$	45.24	UO_2	1.0	PO_4	2.0	H	4.0
$UO_2H_5(PO_4)_2^+$	46.00	UO_2	1.0	PO_4	2.0	H	5.0
HPO_4^{2-}	12.35	PO_4	1.0	H	1.0		
$H_2PO_4^-$	19.55	PO_4	1.0	H	2.0		
H_3PO_4	21.70	PO_4	1.0	H	3.0		
$HMoO_4^-$	4.30	MoO_4	1.0	H	1.0		
HCO_3^-	10.32	CO_3	1.0	H	1.0		
H_2CO_3	16.67	CO_3	1.0	H	2.0		
HSO_4^-	1.99	SO_4	1.0	H	1.0		
OH^-	−13.99	H	−1.0				
			Minerals Allowed to Precipitate				
Calcite	8.48	Ca	1.0	CO_3	1.0		
Gypsum	4.62	Ca	1.0	SO_4	1.0		
$Ca_5(OH)(PO_4)_3$	40.47	Ca	5.0	PO_4	3.0	H	−1.0
$Ca_4(PO_4)_3H$	48.20	Ca	4.0	PO_4	3.0	H	1.0
$CaHPO_4$	19.30	Ca	1.0	PO_4	1.0	H	1.0
Powellite	7.40	Ca	1.0	MoO_4	1.0		
Calcium hydroxide	−21.90	Ca	1.0	H	−2.0		
Uranyl hydroxide	−5.55	UO_2	1.0	H	−2.0		
Schoepite	−5.40	UO_2	1.0	H	−2.0		
Rutherfordine	14.11	UO_2	1.0	CO_3	1.0		
UO_2HPO_4	25.00	UO_2	1.0	PO_4	1.0	H	1.0
$(UO_2)_2H_2(PO_4)_2$	48.09	UO_2	2.0	PO_4	2.0	H	2.0
			Minerals Not Allowed to Precipitate				
Uranyl phosphate		UO_2	3.0	PO_4	2.0		
Calcium	48.61	Ca	1.0	UO_2	2.0	PO_4	2.0

that the trends produced in simulation results presented would be applicable to such sites.

The mill tailings, located at the top (eight elements), were themselves considered to be a boundary in the sense that the total concentrations of the chemical components were set at fixed values; these values were not allowed to deplete during the course of the simulation. The composition of the tailings was 1.5×10^{-1} M for calcium, 10^{-2} M for carbonate, 5×10^{-4} M for uranium, 10^{-8} M for phosphate, 10^{-1} M for sulfate, 3×10^{-2} M for total excess hydronium, and 5×10^{-4} M for molybdate. The initial condition (concentration) of components outside the tailings pile was 2×10^{-2} M, 1.5

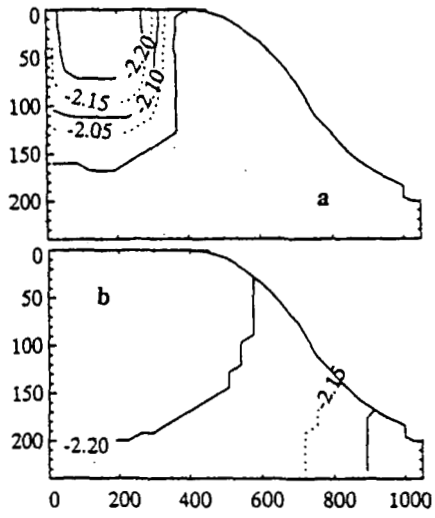

Fig. 12. Distribution of gypsum (log moles) in the system at various times: (*a*) 120 and (*b*) 6000 days.

$\times 10^{-3}$ M, 10^{-7} M, 10^{-8} M, 2×10^{-2} M, 10^{-3} M, and 10^{-6} M for calcium, carbonate, uranium, phosphate, sulfate, hydronium, and molybdate, respectively. For this hypothetical example, the "rain water" was assumed to have the following composition: 10^{-6} M for calcium, 1.5×10^{-5} M for carbonate, 10^{-12} M for uranium, 10^{-8} M for phosphate, 10^{-4} M for sulfate, 10^{-6} M for hydronium, and 10^{-8} M for molybdate.

The simulation was conducted for 7920 days (about 22 years), a time scale of interest in practical problems associated with uranium mill tailings piles. The results of HYDROGEOCHEM simulation were interpolated over a uniform grid. The interpolated results are presented in the form of contour plots. Only the selected highlights of the results are presented.

The release and transport of acidic solutions from the tailings pile alter the *p*H of the system and cause changes in its mineralogy. Figures 10*a*–10*d* show the calculated *p*H through the cross section. Initially, the acidity is confined to the tailings pile, and the *p*H outside the pile is greater than 7; with time the acidic solutions migrate downward and outward, and at 22 years, the groundwater *p*H is significantly acidic near the river. During migration, the acidic solutions are neutralized rapidly as indicated by the closely spaced contours. The neutralization of acidic solutions is also indicated by the gradual disappearance of calcite (Figures 11*a*–11*d*); the decreasing contour values toward the tailings pile indicate the high solubility of calcite in acidic solutions. The migration of acidic solutions is accompanied by spreading of the sulfate plume as shown in Figures 12*a* and 12*b*.

In addition to uranium, uranium mill tailings piles often contain many trace metals including molybdenum, selenium, arsenic, and chromium [*Brookins*, 1984]. The precipitation-dissolution dynamics of molybdenum and uranium, governed by the precipitation of calcium molybdate, uranyl hydroxide, and uranyl carbonate, are examined; all three molybdenum and uranyl solids considered occur as natural minerals, namely, powellite, schoepite and rutherfordine. The precipitation of calcium molybdate developed interesting patterns, sometimes contrary to intuitive expectations. This is caused in response to multiple variations in solution chemical compositions during migration of metal-bearing acidic solutions. Figure 13*a* shows that calcium molybdate precipitation is confined to the tailings pile itself. With release of molybdenum, the molybdate precipitation occurs

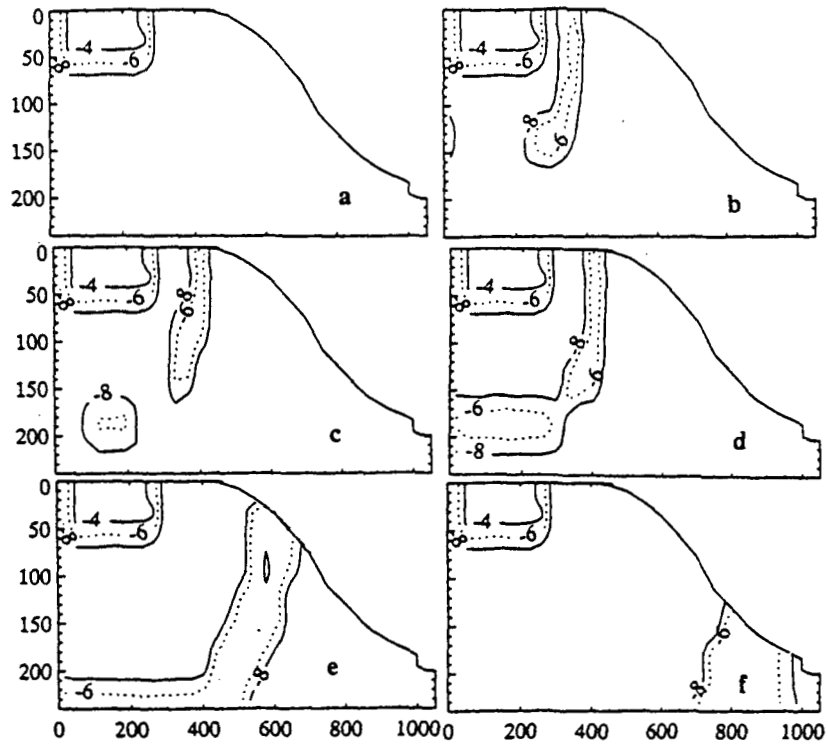

Fig. 13. Distribution of powellite (log moles) in the system at various times: (*a*) 0, (*b*) 520, (*c*) 800, (*d*) 1000, (*e*) 4000, and (*f*) 7290 days.

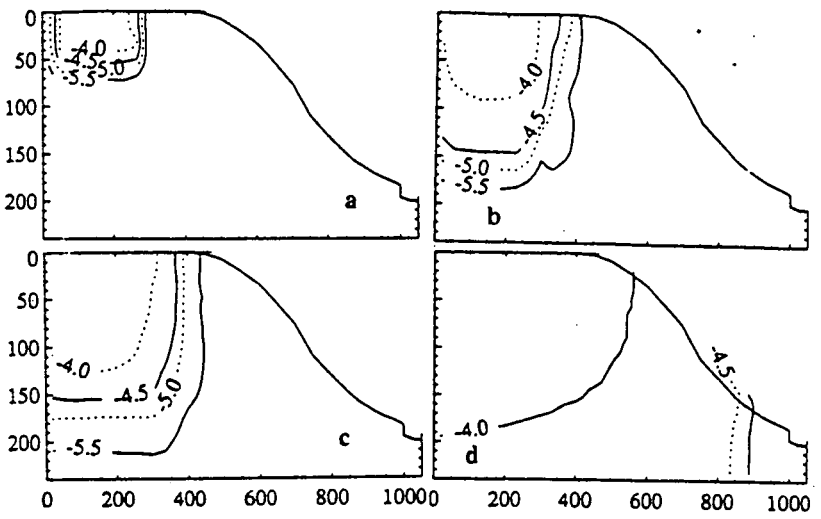

Fig. 14. Distribution of total dissolved molybdate (log moles) in the system at various times: (*a*) 0, (*b*) 520, (*c*) 1000, and (*d*) 7920 days.

outside the tailings pile. Figures 13*b* and 13*c* illustrate development of discontinuous zones of calcium molybdate precipitation at 520 and 800 days, respectively. At 1000 days (Figure 13*d*) the two discontinuous zones of molybdenum precipitation merge and form a band of precipitation surrounding the tailings pile. As the fluids migrate further, the precipitation band widens and itself migrates away from the tailings pile (Figures 13*e* and 13*f*). The precipitation band serves as a natural barrier in retarding migration of molybdenum. As the band of precipitation widens and decreases in intensity, the gradient in molybdenum concentration in the plume becomes markedly less steep (Figures 14*a*–14*d*), indicating a weakening of the barrier effect. Powellite is known to commonly occur in molybdenum-rich soils [*Follett and Barber*, 1967; *Krauskopf*, 1972] and a precipitation-induced natural barrier may influence migration of molybdenum from natural mill tailings. The calculated distribution coefficients (K_d values) vary over 6 orders of magnitude throughout the simulation (Figures 15*a* and 15*b*); once again, a traditional K_d-based solute transport model would have failed to accurately predict the behavior of molybdenum transport in this simple system.

Numerous uranyl solids are possible in the vicinity of mill tailings. To illustrate the role of evolving solution compositions in determining precipitation of solids only three uranyl minerals, a carbonate and two hydroxides, were permitted to precipitate; the precipitation of uranyl phosphates was suppressed. Due to relatively acidic conditions, uranyl solids did not precipitate during the first 4500 days of simulation. Consequently, a uniform, rounded plume of uranium developed in groundwater (Figures 16*a*–16*d*). Small amounts of localized precipitation of rutherfordine occurred at times greater than 4500 days (Figure 17*a*). As in the case of molybdate precipitation, the location and geometry of uranyl precipitation continued to evolve in response to changes in the system's chemical composition (Figures 17*a*–17*d*). Unlike molybdate precipitation, however, the extent of uranyl precipitation was much smaller, and precipitation did not serve as an effective natural barrier for uranium. This is consistent with observations at many uranium mill tailings sites where uranium contamination plumes are much more extensive than the molybdenum plumes (S. Morrison, Chemical-Nuclear Geotech, personal communication, 1991).

The example served to illustrate that HYDROGEOCHEM can simulate many features associated with release of contaminants from uranium mill tailings. It showed the impact of natural chemical processes that retard migration of contaminants, and thus highlighted the importance of designing suitable engineered geochemical barriers for waste sites. The example also illustrated that a K_d computed in laboratory experiments where precipitation may have occurred cannot be used for reliable prediction of contaminant migration in the field because the domain of precipitation is dynamic and governed by interactions among chemical and hydrologic processes.

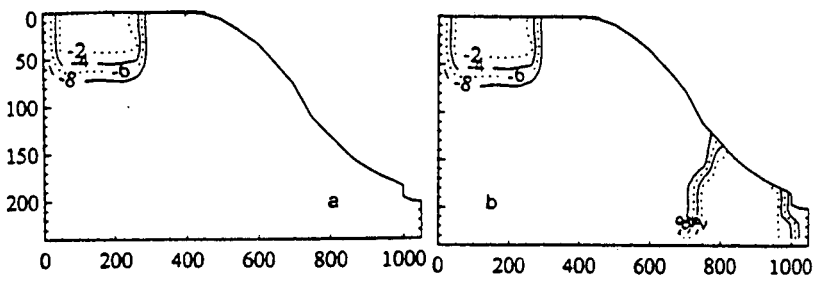

Fig. 15. Variation of calculated K_d (log) at times (*a*) 0 and (*b*) 7290 days.

18

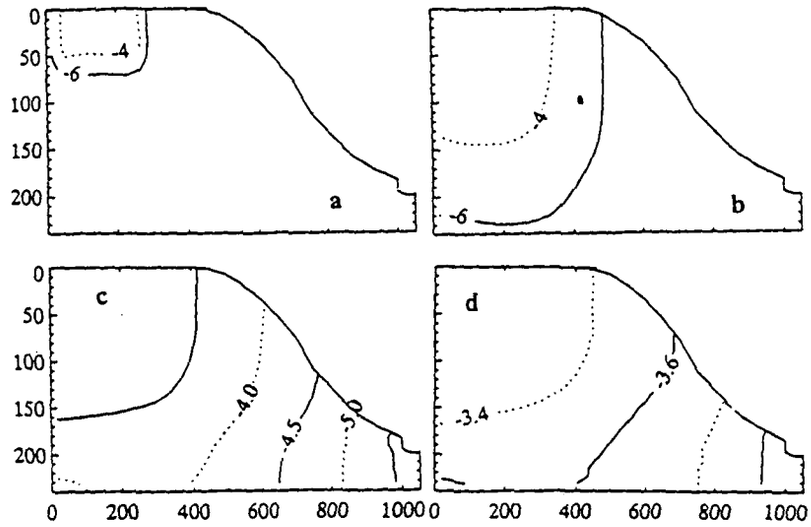

Fig. 16. Distribution of total dissolved uranium (VI) (log moles) in the system at various times: (*a*) 0, (*b*) 520, (*c*) 4000, and (*d*) 7920 days.

CONCLUSIONS

This paper presents a coupled hydrogeochemical model for simulating transport of reactive contaminants in groundwater. The model accounts for chemical processes of complexation, dissolution-precipitation, oxidation-reduction, adsorption including electrical triple layer, and ion exchange during transport through heterogeneous, saturated-unsaturated media under transient or steady state flow conditions. In addition to the mathematical development, a series of examples are presented to demonstrate the capabilities of the model. The selected examples illustrate the model's ability to simulate geochemical evolution in dynamic systems on the one hand, and its utility in solving environmental problems on the other. Examples 2 through 4 exemplify the nonlinearities in the evolution of chemical compositions during reactive transport in dynamic flow-through systems. The example of evolving multifront precipitation-dissolution suggests that chemical processes, including competition among ions and relative thermodynamic stabilities of minerals all must be considered and coupled with transport processes for gaining an insight into a system. The demonstration of the significant errors in computed results by limiting the number of iterations between the hydrologic and the geochemical modules to one, shows that improper coupling of hydrologic and geochemical models can provide misleading results. The relatively simple example of the development of a secondary source of contamination (due to adsorption) that could release, due to desorption, contaminant concentrations thousands of times greater at points away from the original source of contamination shows that investigations aimed at detecting and defining contamination plumes cannot be designed without considering complications that could result from interactions between hydrology and chemistry. The hypothetical mill tailings example illustrates the concept of natural contaminant barriers and illustrates the complex patterns of solid precip-

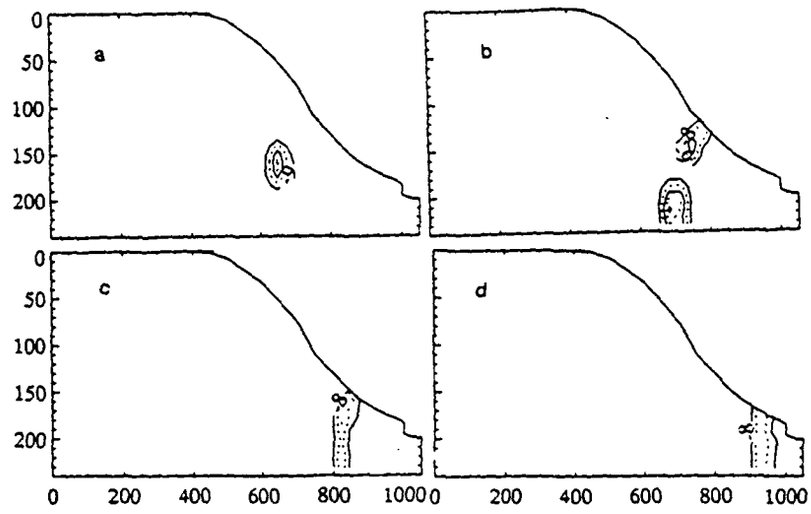

Fig. 17. Distribution of rutherfordine (log moles) in the system at various times: (*a*) 5000, (*b*) 6000, (*c*) 7000, and (*d*) 7920 days.

itation in reactive flow-through chemical systems. Examples 3 and 4 show that calculated K_d values can easily vary over a range of 6 orders of magnitude, and point to the futility of attempts to use distribution coefficient–based or retardation factor–based models for simulating reactive transport.

Acknowledgments. Research was supported by the Subsurface Sciences Program, Ecological Research Division, OHER, U.S. Department of Energy, and certain enhancements were supported by the Office of Civilian Radioactive Waste Management, U.S. Department of Energy, under contract DE-AC05-84OR21400 with Martin Marietta Energy Systems, Inc. The final preparation of this paper was supported by Applied Research Laboratory, Penn State University. V.S.T. wants to thank Science Applications International Corporation for support in preparation of the manuscript and performing the simulations for the revision.

REFERENCES

Brookins, D. G., *Geochemical Aspects of Radioactive Waste Disposal*, 347 pp., Springer-Verlag, New York, 1984.

Bryant, S. L., R. S. Schechter, and L. W. Lake, Interactions of precipitation/dissolution waves and ion exchange in flow through permeable media, *AIChE J.*, *32*(5), 751–764, 1986.

Carnahan, C. L., Simulation of uranium transport with variable temperature and oxidation potential: The computer program THCC, *Rep. 21639*, Lawrence Berkeley Lab., Berkeley, Calif., 1986.

Cederberg, G. A., A groundwater mass transport and equilibrium chemistry model for multicomponent systems, *Water Resour. Res.*, *21*(8), 1095–1104, 1985.

Davies, C. W., *Ion Association*, 190 pp., Butterworth, Stoneham, Mass., 1962.

Davis, J. A., and J. C. Leckie, Surface ionization and complexation at oxide water interface, 2, *J. Colloid Interface Sci.*, *67*, 90–107, 1978.

Follett, R. F., and S. A. Barber, Molybdate phase equilibria in soils, *Soil Sci. Soc. Am. Proc.*, *31*, 26–29, 1967.

Forsythe, G., M. A. Malcolm, and C. B. Moler, *Computer Methods for Mathematical Computations*, 259 pp., Prentice-Hall, Inc., Englewood Cliffs, N. J., 1977.

Grove, D. B., and W. W. Wood, Prediction and field verification of subsurface water quality changes during artificial recharge, Lubbock, Texas, *Ground Water*, *17*(3), 250–257, 1979.

Hostetler, C. J., R. L. Erikson, J. S. Fruchter, and C. T. Kincaid, FASTEHEM package, vol. 1, Overview and application to a chemical transport problem, final report for EPRI EA-5870, Project 2485-2, Pac. Northwest Lab., Richland, Wash., 1989.

Huyakorn, P. S., J. W. Mercer, and D. S. Ward, Finite element matrix and mass balance computational schemes for transport in variably saturated porous media, *Water Resour. Res.*, *21*(3), 346–358, 1985.

Jennings, A. A., D. J. Kirkner, and T. L. Theis, Multicomponent equilibrium chemistry in groundwater quality models, *Water Resour. Res.*, *18*(4), 1089–1096, 1982.

Kirkner, D. J., A. A. Jennings, and T. L. Theis, Multicomponent mass transport with chemical interaction kinetics, *J. Hydrol.*, *76*, 107–117, 1985.

Krauskopf, K. B., Geochemistry of micronutrients, in *Micronutrients in Agriculture*, pp. 7–40, Soil Sciences Society of America, Madison, Wis., 1972.

Lewis, F. M., C. I. Voss, and J. Rubin, Solute transport with equilibrium aqueous complexation and either sorption or ion exchange: Simulation methodology and applications, *J. Hydrol.*, *90*, 81–115, 1987.

Lichtner, P. C., Continuum model for simultaneous chemical reactions and mass transport in hydrothermal systems, *Geochim. Cosmochim. Acta*, *49*, 779–800, 1985.

Liu, C. W., and T. N. Narasimhan, Redox-controlled multiple-species reactive chemical transport, 1, Model development, *Water Resour. Res.*, *25*, 869–882, 1989*a*.

Liu, C. W., and T. N. Narasimhan, Redox-controlled multiple-species reactive chemical transport, 2, Verification and application, *Water Resour. Res.*, *25*, 883–910, 1989*b*.

Morel, F., and J. Morgan, A numerical method for computing equilibria in aqueous chemical systems, *Environ. Sci. Technol.*, *6*(1), 58–67, 1972.

Parkhurst, D. L., D. C. Thorstenson, and L. N. Plummer, PHREEQE—A computer program for geochemical calculations, *U.S. Geol. Surv. Water Resour. Invest.*, *80–96*, 1980.

Reed, M. H., Calculation of multicomponent chemical equilibria and reaction processes in systems involving minerals, gases, and an aqueous phase, *Geochim. Cosmochim. Acta*, *46*, 513–528, 1982.

Rubin, J., Transport of reacting solutes in porous media: Relation between mathematical nature of problem formulation and chemical nature of reactions, *Water Resour. Res.*, *19*(5), 1231–1252, 1983.

Schulz, H. D., and E. J. Reardon, A combined mixing cell/analytical model to describe two-dimensional reactive solute transport for unidirectional groundwater flow, *Water Resour. Res.*, *19*(2), 493–502, 1983.

Stumm, W., and J. J. Morgan, *Aquatic Chemistry, An Introduction Emphasizing Chemical Equilibria in Natural Waters*, 780 pp., John Wiley, New York, 1981.

Tripathi, V. S., Uranium transport modeling: Geochemical data and submodels, Ph.D. dissertation, Stanford Univ., Stanford, Calif., 1983.

Truesdell, A. H., and B. F. Jones, WATEQ, A computer program for calculating chemical equilibria of natural waters, *J. Res. U.S. Geol. Surv.*, *2*(2), 233–248, 1974.

Valocchi, A. J., R. L. Street, and P. V. Roberts, Transport of ion-exchanging solutes in groundwater: Chromatographic theory and field simulation, *Water Resour. Res.*, *17*(5), 1517–1527, 1981.

Walsh, M. P., S. L. Bryant, and L. W. Lake, Precipitation and dissolution of solids attending flow through porous media, *AIChE J.*, *30*(2), 317–328, 1984.

Westall, J. C., J. L. Zachary, and F. M. M. Morel, MINEQL: A computer program for the calculation of chemical equilibrium composition of aqueous system, *Tech. Note 18*, 91 pp., Dep. of Civ. Eng., Mass. Inst. of Technol., Cambridge, 1976.

Wigley, T. M. L., WATSPEC: A computer program for determining the equilibrium speciation of aqueous solutions, *Tech. Bull. Br. Geomorphol. Res. Group*, *20*, 48 pp., 1977.

Wolery, T. J., Calculation of chemical equilibrium between aqueous solution and minerals: The EQ3/6 software package, *Rep. UCRL-52658*, Lawrence Livermore Lab., Livermore, Calif., 1979.

Yeh, G. T., FEMWATER: A finite element model of water flow through saturated-unsatured porous media, 1st revision, *Rep. ORNL-5567/R1*, Oak Ridge Natl. Lab., Oak Ridge, Tenn., 1987.

Yeh, G. T., and D. D. Huff, FEMA: A finite element model of material transport through aquifers, *Rep. ORNL-6063*, Oak Ridge Natl. Lab., Oak Ridge, Tenn., 1985.

Yeh, G. T., and V. S. Tripathi, A critical evaluation of recent developments of hydrogeochemical transport models of reactive multichemical components, *Water Resour. Res.*, *25*(1), 93–108, 1989.

Yeh, G. T., and V. S. Tripathi, HYDROGEOCHEM: A coupled model of hydrological and geochemical equilibrium of multicomponent systems, *Rep. ORNL-6371*, 312 pp., Oak Ridge Natl. Lab., Oak Ridge, Tenn., 1990.

Yeh, G. T., and D. S. Ward, FEMWASTE: A finite element model of WASTE transport model through saturated-unsaturated porous media, *Rep. ORNL-5522*, Oak Ridge Natl. Lab., Oak Ridge, Tenn., 1981.

V. S. Tripathi, Science Applications International Corporation, 1710 Goodridge Drive, McLean, VA 22102.

G.-T. Yeh, Department of Civil Engineering, Penn State University, University Park, PA 16802.

(Received January 28, 1991;
revised July 31, 1991;
accepted August 1, 1991.)

20/20